Draft version May 8, 2023
Typeset using LaTeX default style in AASTeX631

Open data from the third observing run of LIGO, Virgo, KAGRA and GEO

R. Abbott,[1] H. Abe,[2] F. Acernese,[3,4] K. Ackley,[5] S. Adhicary,[6] N. Adhikari,[7] R. X. Adhikari,[1] V. K. Adkins,[8] V. B. Adya,[9] C. Affeldt,[10,11] D. Agarwal,[12] M. Agathos,[13,14] O. D. Aguiar,[15] L. Aiello,[16] A. Ain,[17] P. Ajith,[18] T. Akutsu,[19,20] S. Albanesi,[21,22] R. A. Alfaidi,[23] A. Al-Jodah,[24] C. Alléné,[25] A. Allocca,[26,4] M. Almualla,[27] P. A. Altin,[9] A. Amato,[28,29] L. Amez-Droz,[30] A. Amorosi,[30] S. Anand,[1] A. Ananyeva,[1] R. Andersen,[31] S. B. Anderson,[1] W. G. Anderson,[1] M. Andia,[32] M. Ando,[33] T. Andrade,[34] N. Andres,[25] M. Andrés-Carcasona,[35] T. Andrić,[36] S. Ansoldi,[37,38] J. M. Antelis,[39] S. Antier,[40] M. Aoumi,[41] T. Apostolatos,[42] E. Z. Appavuravther,[43,44] S. Appert,[1] S. K. Apple,[45] K. Arai,[1] A. Araya,[46] M. C. Araya,[1] J. S. Areeda,[47] M. Arène,[48] N. Aritomi,[19] N. Arnaud,[32,49] M. Arogeti,[50] S. M. Aronson,[8] K. G. Arun,[51] H. Asada,[52] G. Ashton,[53] Y. Aso,[19,54] M. Assiduo,[55,56] S. Assis de Souza Melo,[49] S. M. Aston,[57] P. Astone,[58] F. Aubin,[56] K. AultONeal,[39] S. Babak,[48] A. Badalyan,[59] F. Badaracco,[60] C. Badger,[61] S. Bae,[62] S. Bagnasco,[22] Y. Bai,[1] J. G. Baier,[63] L. Baiotti,[64] J. Baird,[48] R. Bajpai,[65] T. Baka,[66] M. Ball,[67] G. Ballardin,[49] S. W. Ballmer,[68] G. Baltus,[69] S. Banagiri,[70] B. Banerjee,[36] D. Bankar,[12] P. Baral,[7] J. C. Barayoga,[1] J. Barber,[16] B. C. Barish,[1] D. Barker,[71] P. Barneo,[34,72] F. Barone,[73,4] B. Barr,[23] L. Barsotti,[74] M. Barsuglia,[48] D. Barta,[75] S. D. Barthelmy,[76] M. A. Barton,[23] I. Bartos,[77] S. Basak,[18] A. Basalaev,[78] R. Bassiri,[79] A. Basti,[80,17] M. Bawaj,[81,43] J. C. Bayley,[23] A. C. Baylor,[7] M. Bazzan,[82,83] B. Bécsy,[84] V. M. Bedakihale,[85] F. Beirnaert,[86] M. Bejger,[87] A. S. Bell,[23] V. Benedetto,[88] D. Beniwal,[89] W. Benoit,[27] J. D. Bentley,[78] M. Ben Yaala,[90] S. Bera,[91] M. Berbel,[92] F. Bergamin,[10,11] B. K. Berger,[79] S. Bernuzzi,[93] M. Beroiz,[1] C. P. L. Berry,[23] D. Bersanetti,[94] A. Bertolini,[29] J. Betzwieser,[57] D. Beveridge,[24] N. Bevins,[95] R. Bhandare,[96] A. V. Bhandari,[12] U. Bhardwaj,[97,29] R. Bhatt,[1] D. Bhattacharjee,[63] S. Bhaumik,[77] A. Bianchi,[29,98] I. A. Bilenko,[99] M. Bilicki,[100] G. Billingsley,[1] S. Bini,[101,102] O. Birnholtz,[103] S. Biscans,[1,74] M. Bischi,[55,56] S. Biscoveanu,[74] A. Bisht,[10,11] B. Biswas,[12] M. Bitossi,[49,17] M.-A. Bizouard,[40] J. K. Blackburn,[1] C. D. Blair,[24,57] D. G. Blair,[24] R. M. Blair,[71] F. Bobba,[104,105] N. Bode,[10,11] M. Boër,[40] G. Bogaert,[40] G. Boileau,[106,40] M. Boldrini,[107,58] G. N. Bolingbroke,[89] L. D. Bonavena,[82] R. Bondarescu,[34] F. Bondu,[108] E. Bonilla,[79] G. S. Bonilla,[47] R. Bonnand,[25] P. Booker,[10,11] R. Bork,[1] V. Boschi,[17] N. Bose,[109] S. Bose,[12] V. Bossilkov,[24] V. Boudart,[69] Y. Bouffanais,[82,83] A. Bozzi,[49] C. Bradaschia,[17] P. R. Brady,[7] M. Braglia,[110] A. Branch,[57] M. Branchesi,[36,111] J. E. Brau,[67] M. Breschi,[93] T. Briant,[112] A. Brillet,[40] M. Brinkmann,[10,11] P. Brockill,[7] A. F. Brooks,[1] J. Brooks,[49] D. D. Brown,[89] S. Brunett,[1] G. Bruno,[60] R. Bruntz,[113] J. Bryant,[114] F. Bucci,[56] J. Buchanan,[113] O. Bulashenko,[34,72] T. Bulik,[115] H. J. Bulten,[29] A. Buonanno,[116,117] K. Burtnyk,[71] R. Buscicchio,[114,118,119] D. Buskulic,[25] C. Buy,[120] R. L. Byer,[79] G. S. Cabourn Davies,[121] G. Cabras,[37,38] R. Cabrita,[60] L. Cadonati,[50] S. Caesar,[16] G. Cagnoli,[122] C. Cahillane,[71] J. Calderón Bustillo,[123] J. D. Callaghan,[23] T. A. Callister,[124,125] E. Calloni,[26,4] J. B. Camp,[76] M. Canepa,[126,94] G. Caneva Santoro,[35] M. Cannavacciuolo,[104] K. C. Cannon,[33] H. Cao,[89] Z. Cao,[127] L. A. Capistran,[128] E. Capocasa,[48] E. Capote,[68] G. Carapella,[104,105] F. Carbognani,[49] M. Carlassara,[10,11] J. B. Carlin,[129] M. Carpinelli,[118,130,49] J. J. Carter,[10,11] G. Carullo,[80,17] J. Casanueva Diaz,[49] C. Casentini,[131,132] G. Castaldi,[133] S. Y. Castro-Lucas,[134] S. Caudill,[29,66] M. Cavaglià,[135] R. Cavalieri,[49] G. Cella,[17] P. Cerdá-Durán,[136] E. Cesarini,[132] W. Chaibi,[40] W. Chakalis,[124,125] S. Chalathadka Subrahmanya,[78] E. Champion,[137] C. Chan,[33] C. L. Chan,[138] K. Chandra,[109] I. P. Chang,[139] W. Chang,[139] P. Chanial,[49,48] S. Chao,[139] C. Chapman-Bird,[23] E. L. Charlton,[113] P. Charlton,[140] E. Chassande-Mottin,[48] L. Chastain,[5] C. Chatterjee,[24] Debarati Chatterjee,[12] Deep Chatterjee,[7] M. Chaturvedi,[96] S. Chaty,[48] K. Chatziioannou,[1] D. Chen,[141] H. Chen,[139] H. Y. Chen,[74] J. Chen,[74] K. H. Chen,[142] X. Chen,[24] Y.-R. Chen,[139] Y. Chen,[143] H. Cheng,[77] P. Chessa,[80,17] H. Y. Cheung,[138] H. Y. Chia,[77] F. Chiadini,[144,105] C-I. Chiang,[145] C. Chiang,[142] G. Chiarini,[83] A. Chiba,[146] R. Chiba,[147] R. Chierici,[148] A. Chincarini,[94] M. L. Chiofalo,[80,17] A. Chiummo,[49] S. Choudhary,[12] N. Christensen,[40] S. S. Y. Chua,[9] K. W. Chung,[61] G. Ciani,[82,83] P. Ciecielag,[87] M. Cieślar,[87] M. Cifaldi,[131,132] A. A. Ciobanu,[89] R. Ciolfi,[149,83] F. Clara,[71] J. A. Clark,[1,50] T. A. Clarke,[5] P. Clearwater,[150] S. Clesse,[151] F. Cleva,[40] E. Coccia,[36,111] E. Codazzo,[36] P.-F. Cohadon,[112] M. Colleoni,[91] C. G. Collette,[30] A. Colombo,[118,119] M. Colpi,[118,119] C. M. Compton,[71] L. Conti,[83] S. J. Cooper,[114] P. Corban,[57] T. R. Corbitt,[8] I. Cordero-Carrión,[152] S. Corezzi,[81,43] N. J. Cornish,[84] A. Corsi,[153] S. Cortese,[49] A. C. Coschizza,[154] R. Cottingham,[57] M. W. Coughlin,[27] J.-P. Coulon,[40] S. T. Countryman,[155] J.-F. Coupechoux,[148] B. Cousins,[6] P. Couvares,[1] D. M. Coward,[24] M. J. Cowart,[57] B. D. Cowburn,[137] D. C. Coyne,[1] R. Coyne,[156] K. Craig,[90] J. D. E. Creighton,[7] T. D. Creighton,[157] A. W. Criswell,[27] J. C. G. Crockett-Gray,[8] M. Croquette,[112] S. G. Crowder,[158] J. R. Cudell,[69] T. J. Cullen,[1] A. Cumming,[23] R. Cummings,[23] E. Cuoco,[49,159,17] M. Curyło,[115] P. Dabadie,[122] T. Dal Canton,[32] S. Dall'Osso,[58] G. Dálya,[86] B. D'Angelo,[126,94] S. Danilishin,[28,29] S. D'Antonio,[132] K. Danzmann,[10,11] K. E. Darroch,[113] C. Darsow-Fromm,[78] A. Dasgupta,[85] L. E. H. Datrier,[23] Sayantani Datta,[51] V. Dattilo,[49] I. Dave,[96] A. Davenport,[134] M. Davier,[32] D. Davis,[1] M. C. Davis,[95] E. J. Daw,[160] M. Dax,[117] D. DeBra,[79,*]

M. Deenadayalan,[12] J. Degallaix,[161] M. De Laurentis,[26,4] S. Deléglise,[112] V. Del Favero,[137] F. De Lillo,[60] N. De Lillo,[23] D. Dell'Aquila,[162,130] W. Del Pozzo,[80,17] F. De Matteis,[131,132] V. D'Emilio,[16] N. Demos,[74] T. Dent,[123] A. Depasse,[60] R. De Pietri,[163,164] R. De Rosa,[26,4] C. De Rossi,[49] R. DeSalvo,[133] R. De Simone,[144] S. Dhurandhar,[12] R. Diab,[77] P. Z. Diamond,[63] M. C. Díaz,[157] N. A. Didio,[68] T. Dietrich,[117] L. Di Fiore,[4] C. Di Fronzo,[30] C. Di Giorgio,[104,105] F. Di Giovanni,[136] M. Di Giovanni,[36] T. Di Girolamo,[26,4] D. Diksha,[29,28] A. Di Lieto,[80,17] A. Di Michele,[81] S. Di Pace,[107,58] I. Di Palma,[107,58] F. Di Renzo,[49,17] Divyajyoti,[165] A. Dmitriev,[114] Z. Doctor,[70] E. Dohmen,[71] P. P. Doleva,[113] L. Donahue,[166] L. D'Onofrio,[26,4] F. Donovan,[74] K. L. Dooley,[16] T. Dooney,[66] S. Doravari,[12] O. Dorosh,[167] M. Drago,[107,58] J. C. Driggers,[71] Y. Drori,[1] J.-G. Ducoin,[168,48] L. Dunn,[129] U. Dupletsa,[36] O. Durante,[104,105] D. D'Urso,[162,130] P.-A. Duverne,[32] S. E. Dwyer,[71] C. Eassa,[71] P. J. Easter,[5] M. Ebersold,[169] T. Eckhardt,[78] G. Eddolls,[23] B. Edelman,[67] T. B. Edo,[1] O. Edy,[121] A. Effler,[57] J. Eichholz,[9] M. Eisenmann,[19] R. A. Eisenstein,[74] A. Ejlli,[16] E. Engelby,[47] A. J. Engl,[79] L. Errico,[26,4] R. C. Essick,[170] H. Estellés,[117] D. Estevez,[171] T. Etzel,[1] C. Evans,[16] M. Evans,[74] T. M. Evans,[57] T. Evstafyeva,[13] B. E. Ewing,[6] F. Fabrizi,[55,56] F. Faedi,[56] V. Fafone,[131,132,36] H. Fair,[68] S. Fairhurst,[16] P. C. Fan,[166] X. Fan,[172] A. M. Farah,[173] B. Farr,[67] W. M. Farr,[124,125] E. J. Fauchon-Jones,[16] G. Favaro,[82] M. Favata,[174] M. Fays,[69] J. Feicht,[1] M. M. Fejer,[79] E. Fenyvesi,[75,175] D. L. Ferguson,[176] A. Fernandez-Galiana,[74] I. Ferrante,[80,17] T. A. Ferreira,[15] F. Fidecaro,[80,17] P. Figura,[115] A. Fiori,[17,80] I. Fiori,[49] M. Fishbach,[70] R. P. Fisher,[113] R. Fittipaldi,[177,105] V. Fiumara,[178,105] R. Flaminio,[25] S. M. Fleischer,[179] L. S. Fleming,[180] E. Floden,[27] H. K. Fong,[33] J. A. Font,[136,181] B. Fornal,[182] P. W. F. Forsyth,[9] A. Franke,[78] S. Frasca,[107,58] F. Frasconi,[17] J. P. Freed,[39] Z. Frei,[183] A. Freise,[29,98] O. Freitas,[184] R. Frey,[67] P. Fritschel,[74] V. V. Frolov,[57] G. G. Fronzé,[22] Y. Fujimoto,[185] I. Fukunaga,[186] P. Fulda,[77] M. Fyffe,[57] H. A. Gabbard,[23] W. E. Gabella,[187] B. U. Gadre,[117,66] K. Gaglani,[39] J. R. Gair,[117] J. Gais,[138] S. Galaudage,[5] S. Gallardo,[188] R. Gamba,[93] D. Ganapathy,[74] A. Ganguly,[12] D. Gao,[79] S. G. Gaonkar,[12] B. Garaventa,[94,126] J. Garcia-Bellido,[110] C. García-Núñez,[180] C. García-Quirós,[91] K. A. Gardner,[154] J. Gargiulo,[49] F. Garufi,[26,4] C. Gasbarra,[131,132] B. Gateley,[71] V. Gayathri,[77,7] G. Gemme,[94] A. Gennai,[17] J. George,[96] O. Gerberding,[78] L. Gergely,[189] S. Ghonge,[50] Abhirup Ghosh,[117] Archisman Ghosh,[86] Shaon Ghosh,[174] Shrobana Ghosh,[16] Tathagata Ghosh,[12] L. Giacoppo,[107,58] J. A. Giaime,[8,57] K. D. Giardina,[57] D. R. Gibson,[180] C. Gier,[90] P. Giri,[17,80] F. Gissi,[88] S. Gkaitatzis,[49] J. Glanzer,[8] A. E. Gleckl,[47] F. Glotin,[32] J. Godfrey,[67] P. Godwin,[1] E. Goetz,[154] R. Goetz,[77] J. Golomb,[1] B. Goncharov,[36] G. González,[8] M. Gosselin,[49] R. Gouaty,[25] D. W. Gould,[9] S. Goyal,[18] B. Grace,[9] A. Grado,[190,4] V. Graham,[23] M. Granata,[161] V. Granata,[104] S. Gras,[74] P. Grassia,[1] C. Gray,[71] R. Gray,[191] G. Greco,[43] A. C. Green,[77] R. Green,[16] S. Green,[121] S. R. Green,[117] A. M. Gretarsson,[39] E. M. Gretarsson,[39] D. Griffith,[1] W. L. Griffiths,[16] H. L. Griggs,[50] G. Grignani,[81,43] A. Grimaldi,[101,102] H. Grote,[16] A. S. Gruson,[47] D. Guerra,[136] D. Guetta,[58] G. M. Guidi,[55,56] A. R. Guimaraes,[8] H. K. Gulati,[85] F. Gulminelli,[192,193] A. M. Gunny,[74] H. Guo,[182] Y. Guo,[29] Anchal Gupta,[1] Anuradha Gupta,[194] Ish Gupta,[6] N. C. Gupta,[85] P. Gupta,[29,66] S. K. Gupta,[109] J. Gurs,[78] Y. Gushima,[195] E. K. Gustafson,[1] N. Gutierrez,[161] F. Guzman,[128] L. Haegel,[48] G. Hain,[113] S. Haino,[145] O. Halim,[38] E. D. Hall,[74] E. Z. Hamilton,[169] G. Hammond,[23] W.-B. Han,[196] M. Haney,[169] J. Hanks,[71] C. Hanna,[6] M. D. Hannam,[16] O. A. Hannuksela,[138,66,29] H. Hansen,[71] J. Hanson,[57] R. Harada,[33] T. Harder,[40] K. Haris,[29,66] T. Harmark,[197] J. Harms,[36,111] G. M. Harry,[45] I. W. Harry,[121] D. Hartwig,[78] B. Haskell,[87] C.-J. Haster,[74] J. S. Hathaway,[137] K. Haughian,[23] H. Hayakawa,[41] K. Hayama,[195] F. J. Hayes,[23] J. Healy,[137] A. Heffernan,[91] A. Heidmann,[112] M. C. Heintze,[57] J. Heinze,[10,11] J. Heinzel,[74] H. Heitmann,[40] F. Hellman,[198] P. Hello,[32] A. F. Helmling-Cornell,[67] G. Hemming,[49] M. Hendry,[23] I. S. Heng,[23] E. Hennes,[29] J.-S. Hennig,[28,29] M. Hennig,[28,29] C. Henshaw,[50] F. Hernandez Vivanco,[5] M. Heurs,[10,11] A. L. Hewitt,[13] S. Higginbotham,[16] S. Hild,[28,29] P. Hill,[90] Y. Himemoto,[199] A. S. Hines,[128] N. Hirata,[19] C. Hirose,[200] J. Ho,[142] S. Hochheim,[10,11] D. Hofman,[161] J. N. Hohmann,[78] D. G. Holcomb,[95] N. A. Holland,[29,98] K. Holley-Bockelmann,[187] I. J. Hollows,[160] Z. J. Holmes,[89] K. Holt,[57] D. E. Holz,[173] Q. Hong,[139] J. Hornung,[67] S. Hoshino,[200] J. Hough,[23] S. Hourihane,[1] D. Howell,[124,125] E. J. Howell,[24] C. G. Hoy,[16,121] D. Hoyland,[114] B.-H. Hsieh,[147] H.-F. Hsieh,[139] C. Hsiung,[201] H. Hsu,[142] P. Hu,[187] Q. Hu,[23] H.-Y. Huang,[145,142] Y.-J. Huang,[6] Y. Huang,[74] Y. T. Huang,[202] M. T. Hübner,[129] A. D. Huddart,[203] B. Hughey,[39] D. C. Y. Hui,[204] V. Hui,[25] S. Husa,[91] S. H. Huttner,[23] R. Huxford,[6] T. Huynh-Dinh,[57] J. Hyland,[23] A. Iakovlev,[205] G. A. Iandolo,[28] B. Idzkowski,[115] A. Iess,[159,17] K. Inayoshi,[206] Y. Inoue,[207] G. Iorio,[82] P. Iosif,[208] J. Irwin,[23] M. Isi,[124,125] M. A. Ismail,[142] Y. Itoh,[186,209] B. R. Iyer,[18] V. JaberianHamedan,[24] T. Jacqmin,[112] P.-E. Jacquet,[112] S. J. Jadhav,[210] S. P. Jadhav,[12] D. Jain,[5] T. Jain,[13] A. L. James,[16] A. Z. Jan,[176] K. Jani,[187] L. Janiurek,[23] J. Janquart,[66,29] K. Janssens,[106,40] N. N. Janthalur,[210] S. Jaraba,[110] P. Jaranowski,[211] S. Jarov,[154] P. Jasal,[34] R. Jaume,[91] W. Javed,[16] A. C. Jenkins,[61] K. Jenner,[89] A. Jennings,[71] W. Jia,[74] J. Jiang,[77] Jian Liu,[24] H.-B. Jin,[212,213] K. Johansmeyer,[174] G. R. Johns,[113] N. A. Johnson,[77] R. Johnston,[23] N. Johny,[10,11] A. W. Jones,[24] D. H. Jones,[9] D. I. Jones,[214] P. Jones,[114] R. Jones,[23] P. Joshi,[6] L. Ju,[24] K. Jung,[215] J. Junker,[10,11] V. Juste,[171] T. Kajita,[216] C. Kalaghatgi,[66,29,217] V. Kalogera,[70] B. Kamai,[1] M. Kamiizumi,[41] N. Kanda,[209,186] S. Kandhasamy,[12] G. Kang,[218] J. B. Kanner,[1] S. J. Kapadia,[18] D. P. Kapasi,[9] S. Karat,[1] C. Karathanasis,[35] S. Karki,[135] D. Kasamatsu,[146] Y. A. Kas-danouche,[59] R. Kashyap,[6] M. Kasprzack,[1] W. Kastaun,[10,11] J. Kato,[146] S. Katsanevas,[49] E. Katsavounidis,[74] J. K. Katsuren,[59] W. Katzman,[57] T. Kaur,[24] K. Kawabe,[71] K. Kawazoe,[195] F. Kéfélian,[40] D. Keitel,[91] I. Kellard,[16] J. Kelley-Derzon,[77]

J. Kennington,[6] J. S. Key,[219] S. Khadka,[79] F. Y. Khalili,[99] S. Khan,[16] T. Khanam,[153] E. A. Khazanov,[205] M. Khursheed,[96] N. Kijbunchoo,[9] C. Kim,[220] J. C. Kim,[221] K. Kim,[220] M. H. Kim,[222] P. Kim,[222] S. Kim,[204] W. S. Kim,[223] Y.-M. Kim,[215] C. Kimball,[70] N. Kimura,[41] M. Kinley-Hanlon,[23] R. Kirchhoff,[10,11] J. S. Kissel,[71] T. Kiyota,[186] S. Klimenko,[77] T. Klinger,[16] A. M. Knee,[154] N. Knust,[10,11] Y. Kobayashi,[185] P. Koch,[10,11] S. M. Koehlenbeck,[10,11] G. Koekoek,[29,28] K. Kohri,[224] K. Kokeyama,[16] S. Koley,[36] N. D. Koliadko,[59] P. Kolitsidou,[16] M. Kolstein,[35] V. Kondrashov,[1] A. K. H. Kong,[139] A. Kontos,[225] M. Korobko,[78] R. V. Kossak,[10,11] N. Kouvatsos,[61] M. Kovalam,[24] N. Koyama,[200] D. B. Kozak,[1] L. Kranzhoff,[10,11] S. L. Kranzhoff,[28,29] V. Kringel,[10,11] N. V. Krishnendu,[10,11] A. Królak,[226,167] G. Kuehn,[10,11] P. Kuijer,[29] M. Kukihara,[195] S. Kulkarni,[194] A. Kumar,[210] Praveen Kumar,[123] Prayush Kumar,[18] Rahul Kumar,[71] Rakesh Kumar,[85] J. Kume,[33] K. Kuns,[74] S. Kuroyanagi,[110,227,228] S. Kuwahara,[33] K. Kwak,[215] G. Lacaille,[23] P. Lagabbe,[25] D. Laghi,[120] M. H. Lakkis,[30] E. Lalande,[229] M. Lalleman,[106] A. Lamberts,[40,230] M. Landry,[71] B. B. Lane,[74] R. N. Lang,[74] J. Lange,[176] B. Lantz,[79] A. La Rana,[58] I. La Rosa,[25] A. Lartaux-Vollard,[32] P. D. Lasky,[5] J. Lawrence,[153] M. Laxen,[57] A. Lazzarini,[1] C. Lazzaro,[82,83] P. Leaci,[107,58] S. Leavey,[10,11] S. LeBohec,[182] Y. K. Lecoeuche,[154] E. Lee,[147] H. M. Lee,[231] H. W. Lee,[221] K. Lee,[222] R.-L. Lee,[14] R. Lee,[74] S. Lee,[232] I. N. Legred,[1] J. Lehmann,[10,11] L. Lehner,[170] A. Lemaître,[233] M. Lenti,[56,234] M. Leonardi,[19] E. Leonova,[97] N. Leroy,[32] N. Letendre,[25] M. Lethuillier,[148] C. Levesque,[229] Y. Levin,[5] K. Leyde,[48] A. K. Y. Li,[1] K. L. Li,[235] T. G. F. Li,[138] X. Li,[143] C.-Y. Lin,[142,236] E. T. Lin,[139] F-K. Lin,[145] F-L. Lin,[237] F. Lin,[142] H. L. Lin,[207] H. Lin,[142] L. C.-C. Lin,[235] F. Linde,[217,29] S. D. Linker,[133,188] T. B. Littenberg,[238] A. Liu,[138] G. C. Liu,[201] F. Llamas,[157] R. K. L. Lo,[1] T. Lo,[139] L. T. London,[74,97] A. Longo,[239] D. Lopez,[169] M. Lopez Portilla,[66] M. Lorenzini,[131,132] V. Loriette,[240] M. Lormand,[57] G. Losurdo,[17] T. P. Lott,[50] J. D. Lough,[10,11] H. A. Loughlin,[74] C. O. Lousto,[137] G. Lovelace,[47] M. J. Lowry,[113] H. Lück,[10,11] D. Lumaca,[131,132] A. P. Lundgren,[121] Y. Lung,[138] A. W. Lussier,[229] J. E. Lynam,[113] L. Ma,[139] S. Ma,[143] M. Ma'arif,[142] R. Macas,[121] M. MacInnis,[74] D. M. Macleod,[16] I. A. O. MacMillan,[1] A. Macquet,[35] I. Magaña Hernandez,[7] C. Magazzù,[17] R. M. Magee,[1] R. Maggiore,[114,29,98] M. Magnozzi,[94,126] M. Mahesh,[78] S. Mahesh,[241] M. Maini,[156] E. Majorana,[107,58] C. N. Makarem,[1] S. Maliakal,[1] A. Malik,[96] N. Man,[40] V. Mandic,[27] V. Mangano,[107,58] B. Mannix,[67] G. L. Mansell,[68,74] G. Mansingh,[45] M. Manske,[7] M. Mantovani,[49] M. Mapelli,[82,83] F. Marchesoni,[44,43,242] D. Marín Pina,[34,72,243] F. Marion,[25] S. Márka,[155] Z. Márka,[155] C. Markakis,[191] A. S. Markosyan,[79] A. Markowitz,[1] E. Maros,[1] A. Marquina,[152] S. Marsat,[120] F. Martelli,[55,56] I. W. Martin,[23] R. M. Martin,[174] B. B. Martinez,[128] M. Martinez,[35] V. A. Martinez,[77] V. Martinez,[122] K. Martinovic,[61] D. V. Martynov,[114] E. J. Marx,[74] H. Masalehdan,[78] K. Mason,[74] A. Masserot,[25] M. Masso Reid,[23] M. Mastrodicasa,[58] S. Mastrogiovanni,[40] M. Mateu-Lucena,[91] M. Matiushechkina,[10,11] K. Matsunaga,[146] N. Mavalvala,[74] R. McCarthy,[71] D. E. McClelland,[9] P. K. McClincy,[6] S. McCormick,[57] L. McCuller,[1] G. I. McGhee,[23] J. McGinn,[23] C. McIsaac,[121] J. McIver,[154] A. McLeod,[24] T. McRae,[9] S. T. McWilliams,[241] D. Meacher,[7] M. Mehmet,[10,11] A. K. Mehta,[117] Q. Meijer,[66] A. Melatos,[129] G. Mendell,[71] A. Menendez-Vazquez,[35] C. S. Menoni,[134] R. A. Mercer,[7] L. Mereni,[161] K. Merfeld,[67] E. L. Merilh,[57] J. D. Merritt,[67] M. Merzougui,[40] C. Messenger,[23] C. Messick,[74] P. M. Meyers,[143] F. Meylahn,[10,11] A. Mhaske,[12] A. Miani,[101,102] H. Miao,[244] I. Michaloliakos,[77] C. Michel,[161] Y. Michimura,[1,33] H. Middleton,[114] D. P. Mihaylov,[117] A. Miller,[188] A. L. Miller,[60] B. Miller,[97,29] S. Miller,[1] M. Millhouse,[50,129] J. C. Mills,[16] E. Milotti,[245,38] Y. Minenkov,[132] N. Mio,[246] Ll. M. Mir,[35] M. Miravet-Tenés,[136] A. Mishra,[12] C. Mishra,[165] T. Mishra,[77] T. Mistry,[160] A. L. Mitchell,[29,98] S. Mitra,[12] V. P. Mitrofanov,[99] G. Mitselmakher,[77] R. Mittleman,[74] O. Miyakawa,[41] S. Miyoki,[41] Geoffrey Mo,[74] L. M. Modafferi,[91] E. Moguel,[63] S. R. P. Mohapatra,[74] S. R. Mohite,[7] M. Molina-Ruiz,[198] C. Mondal,[192] M. Mondin,[188] M. Montani,[55,56] C. J. Moore,[114] J. Moragues,[91] D. Moraru,[71] F. Morawski,[87] A. More,[12] S. More,[12] C. Moreno,[39] G. Moreno,[71] S. Morisaki,[7] Y. Moriwaki,[146] G. Morras,[110] A. Moscatello,[82] B. Mours,[171] C. M. Mow-Lowry,[29,98] S. Mozzon,[121] F. Muciaccia,[107,58] D. Mukherjee,[238] Soma Mukherjee,[157] Subroto Mukherjee,[85] Suvodip Mukherjee,[170,97,247] N. Mukund,[10,11] A. Mullavey,[57] J. Munch,[89] E. A. Muñiz,[68] P. G. Murray,[23] J. Murray-Dean,[16] S. Muusse,[89] S. L. Nadji,[10,11] A. Nagar,[22,248] T. Nagar,[5] N. Nagarajan,[23] K. Nakamura,[19] H. Nakano,[249] M. Nakano,[57] Y. Nakayama,[250] V. Napolano,[49] I. Nardecchia,[131,132] T. Narikawa,[147] H. Narola,[66] L. Naticchioni,[58] R. K. Nayak,[251] B. F. Neil,[24] J. Neilson,[88,105] A. Nelson,[128] T. J. N. Nelson,[57] M. Nery,[10,11] S. Nesseris,[110] A. Neunzert,[219] K. Y. Ng,[74] S. W. S. Ng,[89] C. Nguyen,[48] P. Nguyen,[67] R. Nguyen,[16] T. Nguyen,[74] L. Nguyen Quynh,[252] S. A. Nichols,[8] G. Nieradka,[87] Y. Nishino,[19,253] A. Nishizawa,[33] S. Nissanke,[97,29] E. Nitoglia,[148] W. Niu,[6] F. Nocera,[49] M. Norman,[16] C. North,[16] J. Novak,[254,255,256,257] J. F. Nuño Siles,[110] G. Nurbek,[157] L. K. Nuttall,[121] J. Oberling,[71] J. O'Dell,[203] E. Oelker,[23] M. Oertel,[254,255,256,258,257] G. Oganesyan,[36,111] J. J. Oh,[223] K. Oh,[204] S. H. Oh,[223] T. O'Hanlon,[57] M. Ohashi,[41] T. Ohashi,[185] M. Ohkawa,[200] F. Ohme,[10,11] H. Ohta,[33] A. S. Oliveira,[155] R. Oliveri,[254,255,256] K. Oohara,[259,260] B. O'Reilly,[57] R. G. Ormiston,[27] N. D. Ormsby,[113] M. Orselli,[43,81] R. O'Shaughnessy,[137] E. O'Shea,[261] Y. Oshima,[262] S. Oshino,[41] S. Ossokine,[117] C. Osthelder,[1] D. J. Ottaway,[89] H. Overmier,[57] A. E. Pace,[6] R. Pagano,[8] M. A. Page,[19] A. Pai,[109] S. A. Pai,[96] S. Pal,[251] O. Palashov,[205] M. Pálfi,[183] C. Palomba,[58] K. C. Pan,[139] P. K. Panda,[210] P. T. H. Pang,[29,66] F. Pannarale,[107,58] B. C. Pant,[96] F. H. Panther,[24] F. Paoletti,[17] A. Paoli,[49] A. Paolone,[58,263] E. E. Papalexakis,[31] G. Pappas,[208] A. Parisi,[17,159] J. Park,[232] W. Parker,[57] D. Pascucci,[86] A. Pasqualetti,[49] R. Passaquieti,[80,17] D. Passuello,[17] M. Patel,[113] M. Pathak,[89] A. Patra,[16] B. Patricelli,[80,17] A. S. Patron,[8]

S. Paul,[67] E. Payne,[1] T. Pearce,[16] M. Pedraza,[1] R. Pedurand,[105] R. Pegna,[17,80] M. Pegoraro,[83] A. Pele,[1] F. E. Peña Arellano,[41] S. Penn,[264] A. Perego,[101,102] A. Pereira,[122] C. J. Perez,[71] C. Périgois,[149] C. C. Perkins,[77] A. Perreca,[101,102] S. Perriès,[148] J. W. Perry,[29,98] D. Pesios,[208] J. Petermann,[78] C. Petrillo,[81] H. P. Pfeiffer,[117] H. Pham,[57] K. A. Pham,[27] K. S. Phukon,[29,217] H. Phurailatpam,[138] O. J. Piccinni,[35] M. Pichot,[40] M. Piendibene,[80,17] F. Piergiovanni,[55,56] L. Pierini,[107,58] G. Pierra,[148] V. Pierro,[88,105] G. Pillant,[49] M. Pillas,[32] F. Pilo,[17] L. Pinard,[161] C. Pineda-Bosque,[188] I. M. Pinto,[88,105,265,26,49] B. J. Piotrzkowski,[7] K. Piotrzkowski,[60] M. Pirello,[71] M. D. Pitkin,[13] A. Placidi,[43,81] E. Placidi,[107,58] M. L. Planas,[91] W. Plastino,[266,239] R. Poggiani,[80,17] E. Polini,[25] L. Pompili,[117] D. Y. T. Pong,[138] S. Ponrathnam,[12,†] E. Porcelli,[29] J. Portell,[34,72,243] E. K. Porter,[48] C. Posnansky,[6] R. Poulton,[49] Jade Powell,[150] Jonathan Powell,[16] M. Pracchia,[25] T. Pradier,[171] A. K. Prajapati,[85] K. Prasai,[79] R. Prasanna,[210] G. Pratten,[114] M. Principe,[133,88,265,105] G. A. Prodi,[267,102] L. Prokhorov,[114] P. Prosposito,[131,132] L. Prudenzi,[117] A. Puecher,[29,66] J. Pullin,[8] M. Punturo,[43] F. Puosi,[17,80] P. Puppo,[58] M. Pürrer,[117] H. Qi,[8] V. Quetschke,[157] P. J. Quinonez,[39] R. Quitzow-James,[135] F. J. Raab,[71] G. Raaijmakers,[97,29] N. Radulesco,[40] P. Raffai,[183] S. X. Rail,[229] S. Raja,[96] C. Rajan,[96] K. E. Ramirez,[57] T. D. Ramirez,[47] A. Ramos-Buades,[117] D. Rana,[12] J. Rana,[6] E. Randel,[134] P. R. Rangnekar,[79] P. Rapagnani,[107,58] A. Ray,[7] V. Raymond,[16] N. Raza,[154] M. Razzano,[80,17] J. Read,[47] T. Regimbau,[25] L. Rei,[94] S. Reid,[90] S. W. Reid,[113] D. H. Reitze,[1] P. Relton,[16] A. Renzini,[1] P. Rettegno,[21,22] B. Revenu,[48,268] A. Reza,[29] M. Rezac,[47] A. S. Rezaei,[58,107] F. Ricci,[107,58] D. Richards,[203] J. W. Richardson,[31] A. Rijal,[39] K. Riles,[269] H. K. Riley,[16] S. Rinaldi,[80,17] C. Robertson,[203] N. A. Robertson,[1] F. Robinet,[32] A. Rocchi,[132] S. Rodriguez,[47] L. Rolland,[25] J. G. Rollins,[1] M. Romanelli,[108] R. Romano,[3,4] C. L. Romel,[71] A. Romero,[35] I. M. Romero-Shaw,[5] J. H. Romie,[57] S. Ronchini,[36,111] T. J. Roocke,[89] L. Rosa,[4,26] T. J. Rosauer,[31] C. A. Rose,[7] D. Rosińska,[115] M. P. Ross,[202] M. Rossello,[91] A. Roussel,[16] S. Rowan,[23] S. J. Rowlinson,[114] S. Roy,[66] A. Royzman,[182] D. Rozza,[162,130] P. Ruggi,[49] E. Ruiz Morales,[110] K. Ruiz-Rocha,[187] K. Ryan,[71] S. Sachdev,[7,50] T. Sadecki,[71] J. Sadiq,[123] P. Saffarieh,[29,98] S. S. Saha,[139] S. Saha,[14] Y. Saito,[270] K. Sakai,[271] M. Sakellariadou,[61] T. Sako,[146] S. Sakon,[6] O. S. Salafia,[118,119,272] F. Salces-Carcoba,[1] L. Salconi,[49] M. Saleem,[27] F. Salemi,[101,102] M. Sallé,[29] A. Samajdar,[119] E. J. Sanchez,[1] J. H. Sanchez,[70] L. E. Sanchez,[1] N. Sanchis-Gual,[273,136] J. R. Sanders,[274] A. Sanuy,[34] T. R. Saravanan,[12] N. Sarin,[5] A. Sasli,[208] P. Sassi,[43,81] B. Sassolas,[161] H. Satari,[24] O. Sauter,[77] R. L. Savage,[71] V. Savant,[12] T. Sawada,[209,186] H. L. Sawant,[12] S. Sayah,[161] D. Schaetzl,[1] M. Scheel,[143] S. J. Scherf,[79] J. Scheuer,[70] M. G. Schiworski,[89] P. Schmidt,[114] S. Schmidt,[66] S. J. Schmitz,[63] R. Schnabel,[78] M. Schneewind,[10,11] R. M. S. Schofield,[67] A. Schönbeck,[78] H. Schuler,[6] B. W. Schulte,[10,11] B. F. Schutz,[16,10,11] E. Schwartz,[16] J. Scott,[23] S. M. Scott,[9] T. C. Seetharamu,[23] M. Seglar-Arroyo,[25] Y. Sekiguchi,[275] D. Sellers,[57] A. S. Sengupta,[276] D. Sentenac,[49] E. G. Seo,[138] V. Sequino,[26,4] A. Sergeev,[205] G. Servignat,[255] Y. Setyawati,[66] T. Shaffer,[71] M. S. Shahriar,[70] M. A. Shaikh,[231] B. Shams,[182] L. Shao,[206] P. Sharma,[96] S. Sharma Chaudhary,[135] P. Shawhan,[116] N. S. Shcheblanov,[277,233] A. Sheela,[165] B. Shen,[116] K. G. Shepard,[59] E. Sheridan,[187] Y. Shikano,[278,279] M. Shikauchi,[33] H. Shimizu,[270] K. Shimode,[41] H. Shinkai,[280] D. H. Shoemaker,[74] D. M. Shoemaker,[176] S. ShyamSundar,[96] A. Sider,[30] H. Siegel,[124,125] M. Sieniawska,[60] D. Sigg,[71] L. Silenzi,[43,44] L. P. Singer,[76] D. Singh,[6] M. K. Singh,[18] N. Singh,[115] A. Singha,[28,29] A. M. Sintes,[91] V. Sipala,[162,130] V. Skliris,[16] B. J. J. Slagmolen,[9] T. J. Slaven-Blair,[24] J. Smetana,[114] J. R. Smith,[47] L. Smith,[23] R. J. E. Smith,[5] J. Soldateschi,[234,281,56] S. N. Somala,[282] K. Somiya,[2] K. Soni,[12] S. Soni,[74] V. Sordini,[148] F. Sorrentino,[94] N. Sorrentino,[80,17] H. Sotani,[283] R. Soulard,[40] T. Souradeep,[284,12] E. Sowell,[153] V. Spagnuolo,[28,29] A. P. Spencer,[23] M. Spera,[82,83] P. Spinicelli,[49] A. K. Srivastava,[85] V. Srivastava,[68] C. Stachie,[40] F. Stachurski,[23] D. A. Steer,[48] J. Steinlechner,[28,29] S. Steinlechner,[28,29] N. Stergioulas,[208] M. StPierre,[156] L. C. Strang,[129] G. Stratta,[285,286,58,287] M. D. Strong,[8] A. Strunk,[71] R. Sturani,[288] A. L. Stuver,[95] M. Suchenek,[87] S. Sudhagar,[12] N. Sueltmann,[78] T. Sugiyama,[147] H. G. Suh,[7] A. G. Sullivan,[155] T. Z. Summerscales,[59] L. Sun,[9] S. Sunil,[85] A. Sur,[87] J. Suresh,[33,60] P. J. Sutton,[16] Takamasa Suzuki,[200] Takanori Suzuki,[2] B. L. Swinkels,[29] A. Syx,[171] M. J. Szczepańczyk,[77] P. Szewczyk,[115] M. Tacca,[29] H. Tagoshi,[147] S. C. Tait,[23] H. Takahashi,[289] R. Takahashi,[19] A. Takamori,[46] S. Takano,[262] H. Takeda,[290] M. Takeda,[186] C. J. Talbot,[90] C. Talbot,[74] M. Tamaki,[147] N. Tamanini,[120] D. Tanabe,[142] K. Tanaka,[291] T. Tanaka,[290] A. J. Tanasijczuk,[60] S. Tanioka,[68] D. B. Tanner,[77] D. Tao,[1] L. Tao,[77] R. D. Tapia,[6] E. N. Tapia San Martín,[29] R. Tarafder,[1] C. Taranto,[131] A. Taruya,[292] J. D. Tasson,[166] M. Teloi,[30] R. Tenorio,[91] J. E. S. Terhune,[95] L. Terkowski,[78] H. Themann,[188] M. P. Thirugnanasambandam,[12] L. M. Thomas,[114] M. Thomas,[57] P. Thomas,[71] S. Thomas,[68] J. E. Thompson,[16] S. R. Thondapu,[96] K. A. Thorne,[57] E. Thrane,[5] Shubhanshu Tiwari,[169] Srishti Tiwari,[12] V. Tiwari,[16] A. M. Toivonen,[27] A. E. Tolley,[121] T. Tomaru,[19] K. Tomita,[186] T. Tomura,[41] M. Tonelli,[80,17] A. Torres-Forné,[136] C. I. Torrie,[1] I. Tosta e Melo,[130] E. Tournefier,[25] A. Trapananti,[44,43] F. Travasso,[44,43] G. Traylor,[57] J. Trenado,[34] M. Trevor,[116] M. C. Tringali,[49] A. Tripathee,[269] L. Troiano,[293,105] A. Trovato,[38,245] L. Trozzo,[4] R. J. Trudeau,[1] K. W. Tsang,[29,294,66] T. Tsang,[295] M. Tse,[74] R. Tso,[143] S. Tsuchida,[296] L. Tsukada,[6] T. Tsutsui,[33] K. Turbang,[297,106] M. Turconi,[40] C. Turski,[86] D. Tuyenbayev,[41] H. Ubach,[34,72] A. S. Ubhi,[114] N. Uchikata,[147] T. Uchiyama,[41] R. P. Udall,[1] T. Uehara,[298,299] K. Ueno,[33] C. S. Unnikrishnan,[247] T. Ushiba,[41] A. Utina,[28,29] H. Vahlbruch,[10,11] N. Vaidya,[1] G. Vajente,[1] A. Vajpeyi,[5] G. Valdes,[128] M. Valentini,[101,102] S. Vallero,[22] V. Valsan,[7] N. van Bakel,[29] M. van Beuzekom,[29]

M. van Dael,[29,300] J. F. J. van den Brand,[28,98,29] C. Van Den Broeck,[66,29] D. C. Vander-Hyde,[68] M. van der Sluys,[29,66] A. Van de Walle,[32] J. van Dongen,[29,98] H. van Haevermaet,[106] J. V. van Heijningen,[60] J. Vanosky,[1] M. H. P. M. van Putten,[301] Z. van Ranst,[28] N. van Remortel,[106] M. Vardaro,[217,29] A. F. Vargas,[129] V. Varma,[117] M. Vasúth,[75] A. Vecchio,[114] G. Vedovato,[83] J. Veitch,[23] P. J. Veitch,[89] J. Venneberg,[10,11] G. Venugopalan,[1] P. Verdier,[148] D. Verkindt,[25] P. Verma,[167] Y. Verma,[96] S. M. Vermeulen,[16] D. Veske,[155] F. Vetrano,[55] A. Viceré,[55,56] S. Vidyant,[68] A. D. Viets,[302] A. Vijaykumar,[18] V. Villa-Ortega,[123] M. Vina,[16] E. T. Vincent,[50] J.-Y. Vinet,[40] S. Viret,[148] A. Virtuoso,[245,38] S. Vitale,[74] H. Vocca,[81,43] D. Voigt,[78] E. R. G. von Reis,[71] J. S. A. von Wrangel,[10,11] C. Vorvick,[71] S. P. Vyatchanin,[99] L. E. Wade,[63] M. Wade,[63] K. J. Wagner,[137] R. C. Walet,[29] M. Walker,[113] G. S. Wallace,[90] L. Wallace,[1] H. Wang,[262] J. Z. Wang,[269] W. H. Wang,[157] R. L. Ward,[9] J. Warner,[71] M. Was,[25] T. Washimi,[19] N. Y. Washington,[1] K. Watada,[113] D. Watarai,[33] J. Watchi,[30] K. E. Wayt,[63] B. Weaver,[71] C. R. Weaving,[121] S. A. Webster,[23] M. Weinert,[10,11] A. J. Weinstein,[1] R. Weiss,[74] C. M. Weller,[202] R. A. Weller,[187] F. Wellmann,[10,11] L. Wen,[24] P. Wessels,[10,11] K. Wette,[9] J. T. Whelan,[137] D. D. White,[47] B. F. Whiting,[77] C. Whittle,[74] O. S. Wilk,[63] D. Wilken,[10,11] K. Willetts,[16] D. Williams,[23] M. J. Williams,[23] A. R. Williamson,[121] J. L. Willis,[1] B. Willke,[10,11] C. C. Wipf,[1] G. Woan,[23] J. Woehler,[10,11] J. K. Wofford,[137] D. Wong,[154] H. T. Wong,[142] I. C. F. Wong,[138] M. Wright,[23] C. Wu,[14] D. S. Wu,[10,11] H. Wu,[14] D. M. Wysocki,[7] L. Xiao,[1] V. A. Xu,[74] N. Yadav,[87] T. Yamada,[270] H. Yamamoto,[1] K. Yamamoto,[146] M. Yamamoto,[146] T. Yamamoto,[41] T. S. Yamamoto,[228] K. Yamashita,[250] R. Yamazaki,[303] F. W. Yang,[182] K. Z. Yang,[27] Y.-C. Yang,[139] M. J. Yap,[9] D. W. Yeeles,[16] A. B. Yelikar,[137] T. Y. Yeung,[59] J. Yokoyama,[33] T. Yokozawa,[41] J. Yoo,[261] Hang Yu,[143] Haocun Yu,[74] H. Yuzurihara,[41] A. Zadrożny,[167] A. J. Zannelli,[113] M. Zanolin,[39] M. Zeeshan,[137] S. Zeidler,[304] T. Zelenova,[49] J.-P. Zendri,[83] M. Zevin,[173] J. Zhang,[9] L. Zhang,[1] R. Zhang,[77] T. Zhang,[114] Y. Zhang,[128] C. Zhao,[24] Yue Zhao,[182] Yuhang Zhao,[147,19] Y. Zheng,[135] H. Zhong,[27] R. Zhou,[198] X. J. Zhu,[5] Z.-H. Zhu,[127,172] A. B. Zimmerman,[176] M. E. Zucker,[1,74] J. Zweizig,[1]

The LIGO Scientific Collaboration, the Virgo Collaboration, and the KAGRA Collaboration

[1] *LIGO Laboratory, California Institute of Technology, Pasadena, CA 91125, USA*

[2] *Graduate School of Science, Tokyo Institute of Technology, 2-12-1 Ookayama, Meguro-ku, Tokyo 152-8551, Japan*

[3] *Dipartimento di Farmacia, Università di Salerno, I-84084 Fisciano, Salerno, Italy*

[4] *INFN, Sezione di Napoli, I-80126 Napoli, Italy*

[5] *OzGrav, School of Physics & Astronomy, Monash University, Clayton 3800, Victoria, Australia*

[6] *The Pennsylvania State University, University Park, PA 16802, USA*

[7] *University of Wisconsin-Milwaukee, Milwaukee, WI 53201, USA*

[8] *Louisiana State University, Baton Rouge, LA 70803, USA*

[9] *OzGrav, Australian National University, Canberra, Australian Capital Territory 0200, Australia*

[10] *Max Planck Institute for Gravitational Physics (Albert Einstein Institute), D-30167 Hannover, Germany*

[11] *Leibniz Universität Hannover, D-30167 Hannover, Germany*

[12] *Inter-University Centre for Astronomy and Astrophysics, Pune 411007, India*

[13] *University of Cambridge, Cambridge CB2 1TN, United Kingdom*

[14]

[15] *Instituto Nacional de Pesquisas Espaciais, 12227-010 São José dos Campos, São Paulo, Brazil*

[16] *Cardiff University, Cardiff CF24 3AA, United Kingdom*

[17] *INFN, Sezione di Pisa, I-56127 Pisa, Italy*

[18] *International Centre for Theoretical Sciences, Tata Institute of Fundamental Research, Bengaluru 560089, India*

[19] *Gravitational Wave Science Project, National Astronomical Observatory of Japan, 2-21-1 Osawa, Mitaka City, Tokyo 181-8588, Japan*

[20] *Advanced Technology Center, National Astronomical Observatory of Japan, 2-21-1 Osawa, Mitaka City, Tokyo 181-8588, Japan*

[21] *Dipartimento di Fisica, Università degli Studi di Torino, I-10125 Torino, Italy*

[22] *INFN Sezione di Torino, I-10125 Torino, Italy*

[23] *SUPA, University of Glasgow, Glasgow G12 8QQ, United Kingdom*

[24] *OzGrav, University of Western Australia, Crawley, Western Australia 6009, Australia*

[25] *Univ. Savoie Mont Blanc, CNRS, Laboratoire d'Annecy de Physique des Particules - IN2P3, F-74000 Annecy, France*

[26] *Università di Napoli "Federico II", I-80126 Napoli, Italy*

[27] *University of Minnesota, Minneapolis, MN 55455, USA*

[28] *Maastricht University, 6200 MD Maastricht, Netherlands*

[29] *Nikhef, 1098 XG Amsterdam, Netherlands*

[30] *Université Libre de Bruxelles, Brussels 1050, Belgium*

[31] *University of California, Riverside, Riverside, CA 92521, USA*

[32] *Université Paris-Saclay, CNRS/IN2P3, IJCLab, 91405 Orsay, France*

[33] University of Tokyo, Tokyo, 113-0033, Japan.
[34] Institut de Ciències del Cosmos (ICCUB), Universitat de Barcelona (UB), c. Martí i Franquès, 1, 08028 Barcelona, Spain
[35] Institut de Física d'Altes Energies (IFAE), Barcelona Institute of Science and Technology, and ICREA, E-08193 Barcelona, Spain
[36] Gran Sasso Science Institute (GSSI), I-67100 L'Aquila, Italy
[37] Dipartimento di Scienze Matematiche, Informatiche e Fisiche, Università di Udine, I-33100 Udine, Italy
[38] INFN, Sezione di Trieste, I-34127 Trieste, Italy
[39] Embry-Riddle Aeronautical University, Prescott, AZ 86301, USA
[40] Université Côte d'Azur, Observatoire Côte d'Azur, CNRS, Artemis, F-06304 Nice, France
[41] Institute for Cosmic Ray Research, KAGRA Observatory, The University of Tokyo, 238 Higashi-Mozumi, Kamioka-cho, Hida City, Gifu 506-1205, Japan
[42] Department of Physics, National and Kapodistrian University of Athens, 15771 Ilissia, Greece
[43] INFN, Sezione di Perugia, I-06123 Perugia, Italy
[44] Università di Camerino, I-62032 Camerino, Italy
[45] American University, Washington, DC 20016, USA
[46] Earthquake Research Institute, The University of Tokyo, 1-1-1 Yayoi, Bunkyo-ku, Tokyo 113-0032, Japan
[47] California State University Fullerton, Fullerton, CA 92831, USA
[48] Université Paris Cité, CNRS, Astroparticule et Cosmologie, F-75013 Paris, France
[49] European Gravitational Observatory (EGO), I-56021 Cascina, Pisa, Italy
[50] Georgia Institute of Technology, Atlanta, GA 30332, USA
[51] Chennai Mathematical Institute, Chennai 603103, India
[52] Department of Mathematics and Physics, Graduate School of Science and Technology, Hirosaki University, 3 Bunkyo-cho, Hirosaki, Aomori 036-8561, Japan
[53] Royal Holloway, University of London, London TW20 0EX, United Kingdom
[54] The Graduate University for Advanced Studies (SOKENDAI), 2-21-1 Osawa, Mitaka City, Tokyo 181-8588, Japan
[55] Università degli Studi di Urbino "Carlo Bo", I-61029 Urbino, Italy
[56] INFN, Sezione di Firenze, I-50019 Sesto Fiorentino, Firenze, Italy
[57] LIGO Livingston Observatory, Livingston, LA 70754, USA
[58] INFN, Sezione di Roma, I-00185 Roma, Italy
[59] Andrews University, Berrien Springs, MI 49104, USA
[60] Université catholique de Louvain, B-1348 Louvain-la-Neuve, Belgium
[61] King's College London, University of London, London WC2R 2LS, United Kingdom
[62] Korea Institute of Science and Technology Information, Daejeon 34141, Republic of Korea
[63] Kenyon College, Gambier, OH 43022, USA
[64] International College, Osaka University, 1-1 Machikaneyama-cho, Toyonaka City, Osaka 560-0043, Japan
[65] School of High Energy Accelerator Science, The Graduate University for Advanced Studies (SOKENDAI), 1-1 Oho, Tsukuba City, Ibaraki 305-0801, Japan
[66] Institute for Gravitational and Subatomic Physics (GRASP), Utrecht University, 3584 CC Utrecht, Netherlands
[67] University of Oregon, Eugene, OR 97403, USA
[68] Syracuse University, Syracuse, NY 13244, USA
[69] Université de Liège, B-4000 Liège, Belgium
[70] Northwestern University, Evanston, IL 60208, USA
[71] LIGO Hanford Observatory, Richland, WA 99352, USA
[72] Departament de Física Quàntica i Astrofísica (FQA), Universitat de Barcelona (UB), c. Martí i Franqués, 1, 08028 Barcelona, Spain
[73] Dipartimento di Medicina, Chirurgia e Odontoiatria "Scuola Medica Salernitana", Università di Salerno, I-84081 Baronissi, Salerno, Italy
[74] LIGO Laboratory, Massachusetts Institute of Technology, Cambridge, MA 02139, USA
[75] Wigner RCP, RMKI, H-1121 Budapest, Hungary
[76] NASA Goddard Space Flight Center, Greenbelt, MD 20771, USA
[77] University of Florida, Gainesville, FL 32611, USA
[78] Universität Hamburg, D-22761 Hamburg, Germany
[79] Stanford University, Stanford, CA 94305, USA
[80] Università di Pisa, I-56127 Pisa, Italy
[81] Università di Perugia, I-06123 Perugia, Italy
[82] Università di Padova, Dipartimento di Fisica e Astronomia, I-35131 Padova, Italy
[83] INFN, Sezione di Padova, I-35131 Padova, Italy
[84] Montana State University, Bozeman, MT 59717, USA
[85] Institute for Plasma Research, Bhat, Gandhinagar 382428, India

[86] *Universiteit Gent, B-9000 Gent, Belgium*
[87] *Nicolaus Copernicus Astronomical Center, Polish Academy of Sciences, 00-716, Warsaw, Poland*
[88] *Dipartimento di Ingegneria, Università del Sannio, I-82100 Benevento, Italy*
[89] *OzGrav, University of Adelaide, Adelaide, South Australia 5005, Australia*
[90] *SUPA, University of Strathclyde, Glasgow G1 1XQ, United Kingdom*
[91] *IAC3–IEEC, Universitat de les Illes Balears, E-07122 Palma de Mallorca, Spain*
[92] *Departamento de Matemáticas, Universitat Autònoma de Barcelona, 08193 Bellaterra (Barcelona), Spain*
[93] *Theoretisch-Physikalisches Institut, Friedrich-Schiller-Universität Jena, D-07743 Jena, Germany*
[94] *INFN, Sezione di Genova, I-16146 Genova, Italy*
[95] *Villanova University, Villanova, PA 19085, USA*
[96] *RRCAT, Indore, Madhya Pradesh 452013, India*
[97] *GRAPPA, Anton Pannekoek Institute for Astronomy and Institute for High-Energy Physics, University of Amsterdam, 1098 XH Amsterdam, Netherlands*
[98] *Department of Physics and Astronomy, Vrije Universiteit Amsterdam, 1081 HV Amsterdam, Netherlands*
[99] *Lomonosov Moscow State University, Moscow 119991, Russia*
[100] *Center for Theoretical Physics, Polish Academy of Sciences, 02-668, Warsaw, Poland*
[101] *Università di Trento, Dipartimento di Fisica, I-38123 Povo, Trento, Italy*
[102] *INFN, Trento Institute for Fundamental Physics and Applications, I-38123 Povo, Trento, Italy*
[103] *Bar-Ilan University, Ramat Gan, 5290002, Israel*
[104] *Dipartimento di Fisica "E.R. Caianiello", Università di Salerno, I-84084 Fisciano, Salerno, Italy*
[105] *INFN, Sezione di Napoli, Gruppo Collegato di Salerno, I-80126 Napoli, Italy*
[106] *Universiteit Antwerpen, 2000 Antwerpen, Belgium*
[107] *Università di Roma "La Sapienza", I-00185 Roma, Italy*
[108] *Univ Rennes, CNRS, Institut FOTON - UMR 6082, F-35000 Rennes, France*
[109] *Indian Institute of Technology Bombay, Powai, Mumbai 400 076, India*
[110] *Instituto de Fisica Teorica UAM-CSIC, Universidad Autonoma de Madrid, 28049 Madrid, Spain*
[111] *INFN, Laboratori Nazionali del Gran Sasso, I-67100 Assergi, Italy*
[112] *Laboratoire Kastler Brossel, Sorbonne Université, CNRS, ENS-Université PSL, Collège de France, F-75005 Paris, France*
[113] *Christopher Newport University, Newport News, VA 23606, USA*
[114] *University of Birmingham, Birmingham B15 2TT, United Kingdom*
[115] *Astronomical Observatory Warsaw University, 00-478 Warsaw, Poland*
[116] *University of Maryland, College Park, MD 20742, USA*
[117] *Max Planck Institute for Gravitational Physics (Albert Einstein Institute), D-14476 Potsdam, Germany*
[118] *Università degli Studi di Milano-Bicocca, I-20126 Milano, Italy*
[119] *INFN, Sezione di Milano-Bicocca, I-20126 Milano, Italy*
[120] *L2IT, Laboratoire des 2 Infinis - Toulouse, Université de Toulouse, CNRS/IN2P3, UPS, F-31062 Toulouse Cedex 9, France*
[121] *University of Portsmouth, Portsmouth, PO1 3FX, United Kingdom*
[122] *Université de Lyon, Université Claude Bernard Lyon 1, CNRS, Institut Lumière Matière, F-69622 Villeurbanne, France*
[123] *IGFAE, Universidade de Santiago de Compostela, 15782 Spain*
[124] *Stony Brook University, Stony Brook, NY 11794, USA*
[125] *Center for Computational Astrophysics, Flatiron Institute, New York, NY 10010, USA*
[126] *Dipartimento di Fisica, Università degli Studi di Genova, I-16146 Genova, Italy*
[127] *Department of Astronomy, Beijing Normal University, Xinjiekouwai Street 19, Haidian District, Beijing 100875, China*
[128] *Texas A&M University, College Station, TX 77843, USA*
[129] *OzGrav, University of Melbourne, Parkville, Victoria 3010, Australia*
[130] *INFN, Laboratori Nazionali del Sud, I-95125 Catania, Italy*
[131] *Università di Roma Tor Vergata, I-00133 Roma, Italy*
[132] *INFN, Sezione di Roma Tor Vergata, I-00133 Roma, Italy*
[133] *University of Sannio at Benevento, I-82100 Benevento, Italy and INFN, Sezione di Napoli, I-80100 Napoli, Italy*
[134] *Colorado State University, Fort Collins, CO 80523, USA*
[135] *Missouri University of Science and Technology, Rolla, MO 65409, USA*
[136] *Departamento de Astronomía y Astrofísica, Universitat de València, E-46100 Burjassot, València, Spain*
[137] *Rochester Institute of Technology, Rochester, NY 14623, USA*
[138] *The Chinese University of Hong Kong, Shatin, NT, Hong Kong*
[139] *National Tsing Hua University, Hsinchu City, 30013 Taiwan*
[140] *OzGrav, Charles Sturt University, Wagga Wagga, New South Wales 2678, Australia*
[141] *Kamioka Branch, National Astronomical Observatory of Japan, 238 Higashi-Mozumi, Kamioka-cho, Hida City, Gifu 506-1205, Japan*

[142] National Central University, Taoyuan City 320317, Taiwan
[143] CaRT, California Institute of Technology, Pasadena, CA 91125, USA
[144] Dipartimento di Ingegneria Industriale (DIIN), Università di Salerno, I-84084 Fisciano, Salerno, Italy
[145] Institute of Physics, Academia Sinica, 128 Sec. 2, Academia Rd., Nankang, Taipei 11529, Taiwan
[146] Faculty of Science, University of Toyama, 3190 Gofuku, Toyama City, Toyama 930-8555, Japan
[147] Institute for Cosmic Ray Research, KAGRA Observatory, The University of Tokyo, 5-1-5 Kashiwa-no-Ha, Kashiwa City, Chiba 277-8582, Japan
[148] Université Lyon, Université Claude Bernard Lyon 1, CNRS, IP2I Lyon / IN2P3, UMR 5822, F-69622 Villeurbanne, France
[149] INAF, Osservatorio Astronomico di Padova, I-35122 Padova, Italy
[150] OzGrav, Swinburne University of Technology, Hawthorn VIC 3122, Australia
[151] Université libre de Bruxelles, 1050 Bruxelles, Belgium
[152] Departamento de Matemáticas, Universitat de València, E-46100 Burjassot, València, Spain
[153] Texas Tech University, Lubbock, TX 79409, USA
[154] University of British Columbia, Vancouver, BC V6T 1Z4, Canada
[155] Columbia University, New York, NY 10027, USA
[156] University of Rhode Island, Kingston, RI 02881, USA
[157] The University of Texas Rio Grande Valley, Brownsville, TX 78520, USA
[158] Bellevue College, Bellevue, WA 98007, USA
[159] Scuola Normale Superiore, I-56126 Pisa, Italy
[160] The University of Sheffield, Sheffield S10 2TN, United Kingdom
[161] Université Lyon, Université Claude Bernard Lyon 1, CNRS, Laboratoire des Matériaux Avancés (LMA), IP2I Lyon / IN2P3, UMR 5822, F-69622 Villeurbanne, France
[162] Università degli Studi di Sassari, I-07100 Sassari, Italy
[163] Dipartimento di Scienze Matematiche, Fisiche e Informatiche, Università di Parma, I-43124 Parma, Italy
[164] INFN, Sezione di Milano Bicocca, Gruppo Collegato di Parma, I-43124 Parma, Italy
[165] Indian Institute of Technology Madras, Chennai 600036, India
[166] Carleton College, Northfield, MN 55057, USA
[167] National Center for Nuclear Research, 05-400 Świerk-Otwock, Poland
[168] Institut d'Astrophysique de Paris, Sorbonne Université, CNRS, UMR 7095, 75014 Paris, France
[169] University of Zurich, Winterthurerstrasse 190, 8057 Zurich, Switzerland
[170] Perimeter Institute, Waterloo, ON N2L 2Y5, Canada
[171] Université de Strasbourg, CNRS, IPHC UMR 7178, F-67000 Strasbourg, France
[172] School of Physics and Technology, Wuhan University, Bayi Road 299, Wuchang District, Wuhan, Hubei, 430072, China
[173] University of Chicago, Chicago, IL 60637, USA
[174] Montclair State University, Montclair, NJ 07043, USA
[175] Institute for Nuclear Research, H-4026 Debrecen, Hungary
[176] University of Texas, Austin, TX 78712, USA
[177] CNR-SPIN, I-84084 Fisciano, Salerno, Italy
[178] Scuola di Ingegneria, Università della Basilicata, I-85100 Potenza, Italy
[179] Western Washington University, Bellingham, WA 98225, USA
[180] SUPA, University of the West of Scotland, Paisley PA1 2BE, United Kingdom
[181] Observatori Astronòmic, Universitat de València, E-46980 Paterna, València, Spain
[182] The University of Utah, Salt Lake City, UT 84112, USA
[183] Eötvös University, Budapest 1117, Hungary
[184] Centro de Física das Universidades do Minho e do Porto, Universidade do Minho, PT-4710-057 Braga, Portugal
[185] Department of Physics, Graduate School of Science, Osaka City University, 3-3-138 Sugimoto-cho, Sumiyoshi-ku, Osaka City, Osaka 558-8585, Japan
[186] Department of Physics, Graduate School of Science, Osaka Metropolitan University, 3-3-138 Sugimoto-cho, Sumiyoshi-ku, Osaka City, Osaka 558-8585, Japan
[187] Vanderbilt University, Nashville, TN 37235, USA
[188] California State University, Los Angeles, Los Angeles, CA 90032, USA
[189] University of Szeged, Dóm tér 9, Szeged 6720, Hungary
[190] INAF, Osservatorio Astronomico di Capodimonte, I-80131 Napoli, Italy
[191] Queen Mary University of London, London E1 4NS, United Kingdom
[192] Université de Normandie, ENSICAEN, UNICAEN, CNRS/IN2P3, LPC Caen, F-14000 Caen, France
[193] Laboratoire de Physique Corpusculaire Caen, 6 boulevard du maréchal Juin, F-14050 Caen, France
[194] The University of Mississippi, University, MS 38677, USA

[195] *Department of Applied Physics, Fukuoka University, 8-19-1 Nanakuma, Jonan, Fukuoka City, Fukuoka 814-0180, Japan*
[196] *Shanghai Astronomical Observatory, Chinese Academy of Sciences, 80 Nandan Road, Shanghai 200030, China*
[197] *Niels Bohr Institute, Copenhagen University, 2100 København, Denmark*
[198] *University of California, Berkeley, CA 94720, USA*
[199] *College of Industrial Technology, Nihon University, 1-2-1 Izumi, Narashino City, Chiba 275-8575, Japan*
[200] *Faculty of Engineering, Niigata University, 8050 Ikarashi-2-no-cho, Nishi-ku, Niigata City, Niigata 950-2181, Japan*
[201] *Department of Physics, Tamkang University, No. 151, Yingzhuan Rd., Danshui Dist., New Taipei City 25137, Taiwan*
[202] *University of Washington, Seattle, WA 98195, USA*
[203] *Rutherford Appleton Laboratory, Didcot OX11 0DE, United Kingdom*
[204] *Department of Astronomy and Space Science, Chungnam National University, 9 Daehak-ro, Yuseong-gu, Daejeon 34134, Republic of Korea*
[205] *Institute of Applied Physics, Nizhny Novgorod, 603950, Russia*
[206] *Kavli Institute for Astronomy and Astrophysics, Peking University, Yiheyuan Road 5, Haidian District, Beijing 100871, China*
[207] *Department of Physics, Center for High Energy and High Field Physics, National Central University, No.300, Zhongda Rd, Zhongli District, Taoyuan City 32001, Taiwan*
[208] *Department of Physics, Aristotle University of Thessaloniki, 54124 Thessaloniki, Greece*
[209] *Nambu Yoichiro Institute of Theoretical and Experimental Physics, Osaka Metropolitan University, 3-3-138 Sugimoto-cho, Sumiyoshi-ku, Osaka City, Osaka 558-8585, Japan*
[210] *Directorate of Construction, Services & Estate Management, Mumbai 400094, India*
[211] *University of Białystok, 15-424 Białystok, Poland*
[212] *National Astronomical Observatories, Chinese Academic of Sciences, 20A Datun Road, Chaoyang District, Beijing, China*
[213] *School of Astronomy and Space Science, University of Chinese Academy of Sciences, 20A Datun Road, Chaoyang District, Beijing, China*
[214] *University of Southampton, Southampton SO17 1BJ, United Kingdom*
[215] *Department of Physics, Ulsan National Institute of Science and Technology, 50 UNIST-gil, Ulju-gun, Ulsan 44919, Republic of Korea*
[216] *Institute for Cosmic Ray Research, The University of Tokyo, 5-1-5 Kashiwa-no-Ha, Kashiwa City, Chiba 277-8582, Japan*
[217] *Institute for High-Energy Physics, University of Amsterdam, 1098 XH Amsterdam, Netherlands*
[218] *Chung-Ang University, Seoul 06974, Republic of Korea*
[219] *University of Washington Bothell, Bothell, WA 98011, USA*
[220] *Ewha Womans University, Seoul 03760, Republic of Korea*
[221] *Inje University Gimhae, South Gyeongsang 50834, Republic of Korea*
[222] *Sungkyunkwan University, Seoul 03063, Republic of Korea*
[223] *National Institute for Mathematical Sciences, Daejeon 34047, Republic of Korea*
[224] *Institute of Particle and Nuclear Studies, High Energy Accelerator Research Organization (KEK), 1-1 Oho, Tsukuba City, Ibaraki 305-0801, Japan*
[225] *Bard College, Annandale-On-Hudson, NY 12504, USA*
[226] *Institute of Mathematics, Polish Academy of Sciences, 00656 Warsaw, Poland*
[227] *Instituto de Física Teórica UAM-CSIC, Universidad Autonóma de Madrid, C/ Nicolas Cabrera, 13-15, 28049 Madrid, Spain*
[228] *Department of Physics, Nagoya University, ES building, Furocho, Chikusa-ku, Nagoya, Aichi 464-8602, Japan*
[229] *Université de Montréal/Polytechnique, Montreal, Quebec H3T 1J4, Canada*
[230] *Université Côte d'Azur, Observatoire Côte d'Azur, CNRS, Lagrange, F-06304 Nice, France*
[231] *Seoul National University, Seoul 08826, Republic of Korea*
[232] *Technology Center for Astronomy and Space Science, Korea Astronomy and Space Science Institute, 776 Daedeokdae-ro, Yuseong-gu, Daejeon 34055, Republic of Korea*
[233] *NAVIER, École des Ponts, Univ Gustave Eiffel, CNRS, Marne-la-Vallée, France*
[234] *Università di Firenze, Sesto Fiorentino I-50019, Italy*
[235] *Department of Physics, National Cheng Kung University, No.1, University Road, Tainan City 701, Taiwan*
[236] *National Center for High-performance computing, National Applied Research Laboratories, No. 7, R&D 6th Rd., Hsinchu Science Park, Hsinchu City 30076, Taiwan*
[237] *Department of Physics, National Taiwan Normal University, 88 Ting-Chou Rd., sec. 4, Taipei 116, Taiwan*
[238] *NASA Marshall Space Flight Center, Huntsville, AL 35811, USA*
[239] *INFN, Sezione di Roma Tre, I-00146 Roma, Italy*
[240] *ESPCI, CNRS, F-75005 Paris, France*
[241] *West Virginia University, Morgantown, WV 26506, USA*
[242] *School of Physics Science and Engineering, Tongji University, Shanghai 200092, China*
[243] *Institut d'Estudis Espacials de Catalunya, c. Gran Capità, 2-4, 08034 Barcelona, Spain*
[244] *Tsinghua University, Beijing 100084, China*
[245] *Dipartimento di Fisica, Università di Trieste, I-34127 Trieste, Italy*

[246] *Institute for Photon Science and Technology, The University of Tokyo, 2-11-16 Yayoi, Bunkyo-ku, Tokyo 113-8656, Japan*
[247] *Tata Institute of Fundamental Research, Mumbai 400005, India*
[248] *Institut des Hautes Etudes Scientifiques, F-91440 Bures-sur-Yvette, France*
[249] *Faculty of Law, Ryukoku University, 67 Fukakusa Tsukamoto-cho, Fushimi-ku, Kyoto City, Kyoto 612-8577, Japan*
[250] *Graduate School of Science and Engineering, University of Toyama, 3190 Gofuku, Toyama City, Toyama 930-8555, Japan*
[251] *Indian Institute of Science Education and Research, Kolkata, Mohanpur, West Bengal 741252, India*
[252] *Department of Physics and Astronomy, University of Notre Dame, 225 Nieuwland Science Hall, Notre Dame, IN 46556, USA*
[253] *Department of Astronomy, The University of Tokyo, 7-3-1 Hongo, Bunkyo-ku, Tokyo 113-0033, Japan*
[254] *Centre national de la recherche scientifique, 75016 Paris, France*
[255] *Laboratoire Univers et Théories, Observatoire de Paris, 92190 Meudon, France*
[256] *Observatoire de Paris, 75014 Paris, France*
[257] *Université PSL, 75006 Paris, France*
[258] *Université de Paris Cité, 75006 Paris, France*
[259] *Graduate School of Science and Technology, Niigata University, 8050 Ikarashi-2-no-cho, Nishi-ku, Niigata City, Niigata 950-2181, Japan*
[260] *Niigata Study Center, the Open University of Japan, 754 Ichibancho, Asahimachi-dori, Chuo-ku, Niigata City, Niigata 951-8122, Japan*
[261] *Cornell University, Ithaca, NY 14850, USA*
[262] *Department of Physics, The University of Tokyo, 7-3-1 Hongo, Bunkyo-ku, Tokyo 113-0033, Japan*
[263] *Consiglio Nazionale delle Ricerche - Istituto dei Sistemi Complessi, I-00185 Roma, Italy*
[264] *Hobart and William Smith Colleges, Geneva, NY 14456, USA*
[265] *Museo Storico della Fisica e Centro Studi e Ricerche "Enrico Fermi", I-00184 Roma, Italy*
[266] *Dipartimento di Matematica e Fisica, Università degli Studi Roma Tre, I-00146 Roma, Italy*
[267] *Università di Trento, Dipartimento di Matematica, I-38123 Povo, Trento, Italy*
[268] *Subatech, CNRS/IN2P3 - Institut Mines-Telecom Atlantique - Université de Nantes, 4 rue Alfred Kastler BP 20722 44307 Nantes C'EDEX 03, France*
[269] *University of Michigan, Ann Arbor, MI 48109, USA*
[270] *Accelerator Laboratory, High Energy Accelerator Research Organization (KEK), 1-1 Oho, Tsukuba City, Ibaraki 305-0801, Japan*
[271] *Department of Electronic Control Engineering, National Institute of Technology, Nagaoka College, 888 Nishikatakai, Nagaoka City, Niigata 940-8532, Japan*
[272] *INAF, Osservatorio Astronomico di Brera sede di Merate, I-23807 Merate, Lecco, Italy*
[273] *Departamento de Matemática da Universidade de Aveiro and Centre for Research and Development in Mathematics and Applications, 3810-183 Aveiro, Portugal*
[274] *Marquette University, Milwaukee, WI 53233, USA*
[275] *Faculty of Science, Toho University, 2-2-1 Miyama, Funabashi City, Chiba 274-8510, Japan*
[276] *Indian Institute of Technology, Palaj, Gandhinagar, Gujarat 382355, India*
[277] *Laboratoire MSME, Cité Descartes, 5 Boulevard Descartes, Champs-sur-Marne, 77454 Marne-la-Vallée Cedex 2, France*
[278] *Graduate School of Science and Technology, Gunma University, 4-2 Aramaki, Maebashi, Gunma 371-8510, Japan*
[279] *Institute for Quantum Studies, Chapman University, 1 University Dr., Orange, CA 92866, USA*
[280] *Faculty of Information Science and Technology, Osaka Institute of Technology, 1-79-1 Kitayama, Hirakata City, Osaka 573-0196, Japan*
[281] *INAF, Osservatorio Astrofisico di Arcetri, I-50125 Firenze, Italy*
[282] *Indian Institute of Technology Hyderabad, Sangareddy, Khandi, Telangana 502285, India*
[283] *Interdisciplinary Theoretical and Mathematical Sciences Program (iTHEMS), The Institute of Physical and Chemical Research (RIKEN), 2-1 Hirosawa, Wako, Saitama 351-0198, Japan*
[284] *Indian Institute of Science Education and Research, Pune, Maharashtra 411008, India*
[285] *Institut für Theoretische Physik, Johann Wolfgang Goethe-Universität, Max-von-Laue-Str. 1, 60438 Frankfurt am Main, Germany*
[286] *Istituto di Astrofisica e Planetologia Spaziali di Roma, 00133 Roma, Italy*
[287] *INAF, Osservatorio di Astrofisica e Scienza dello Spazio, I-40129 Bologna, Italy*
[288] *Universidade Estadual Paulista, 01140-070 Campinas, São Paulo, Brazil*
[289] *Research Center for Space Science, Advanced Research Laboratories, Tokyo City University, 8-15-1 Todoroki, Setagaya, Tokyo 158-0082, Japan*
[290] *Department of Physics, Kyoto University, Kita-Shirakawa Oiwake-cho, Sakyou-ku, Kyoto City, Kyoto 606-8502, Japan*
[291] *Institute for Cosmic Ray Research, Research Center for Cosmic Neutrinos, The University of Tokyo, 5-1-5 Kashiwa-no-Ha, Kashiwa City, Chiba 277-8582, Japan*
[292] *Yukawa Institute for Theoretical Physics, Kyoto University, Kita-Shirakawa Oiwake-cho, Sakyou-ku, Kyoto City, Kyoto 606-8502, Japan*

[293] Dipartimento di Scienze Aziendali - Management and Innovation Systems (DISA-MIS), Università di Salerno, I-84084 Fisciano, Salerno, Italy
[294] Van Swinderen Institute for Particle Physics and Gravity, University of Groningen, 9747 AG Groningen, Netherlands
[295] Faculty of Science, Department of Physics, The Chinese University of Hong Kong, Shatin, N.T., Hong Kong
[296] National Institute of Technology, Fukui College, Geshi-cho, Sabae-shi, Fukui 916-8507, Japan
[297] Vrije Universiteit Brussel, 1050 Brussel, Belgium
[298] Department of Communications Engineering, National Defense Academy of Japan, 1-10-20 Hashirimizu, Yokosuka City, Kanagawa 239-8686, Japan
[299] Department of Physics, University of Florida, Gainesville, FL 32611, USA
[300] Eindhoven University of Technology, 5600 MB Eindhoven, Netherlands
[301] Department of Physics and Astronomy, Sejong University, 209 Neungdong-ro, Gwangjin-gu, Seoul 143-747, Republic of Korea
[302] Concordia University Wisconsin, Mequon, WI 53097, USA
[303] Department of Physical Sciences, Aoyama Gakuin University, 5-10-1 Fuchinobe, Sagamihara City, Kanagawa 252-5258, Japan
[304] Department of Physics, Rikkyo University, 3-34-1 Nishiikebukuro, Toshima-ku, Tokyo 171-8501, Japan

ABSTRACT

The global network of gravitational-wave observatories now includes five detectors, namely LIGO Hanford, LIGO Livingston, Virgo, KAGRA, and GEO 600. These detectors collected data during their third observing run, O3, composed of three phases: O3a starting in April of 2019 and lasting six months, O3b starting in November of 2019 and lasting five months, and O3GK starting in April of 2020 and lasting 2 weeks. In this paper we describe these data and various other science products that can be freely accessed through the Gravitational Wave Open Science Center at https://gwosc.org. The main dataset, consisting of the gravitational-wave strain time series that contains the astrophysical signals, is released together with supporting data useful for their analysis and documentation, tutorials, as well as analysis software packages.

1. INTRODUCTION

Gravitational-wave (GW) detectors develop through successive generations of instruments with increasing sensitivity (Abbott et al. 2020a). The US-based Advanced LIGO[1] detectors (Aasi et al. 2015) were the first two instruments of the current generation to begin operation, collecting data during the first observing run (O1) from September 2015 to January 2016, including the first direct detection of gravitational waves (Abbott et al. 2016). The second observing run (O2) followed from November 2016 to August 2017, with the European detector Advanced Virgo (Acernese et al. 2015) joining in August 2017. The GEO 600 detector in Germany (Dooley et al. 2016) serves as a center of research and development, and is used to test a number of critical detector technologies. Another GW detector, the Japan-based KAGRA (Akutsu et al. 2021), has also been rapidly developing.

This article focuses on the data collected during the third observing run, O3, that took place from April 1 2019 to April 21 2020. The bulk of this observing run collected data only from LIGO and Virgo, and is divided into two main operational phases: O3a from April 1 2019 to October 1 2019, and O3b from November 1 2019 to March 27 2020, with a one-month maintenance break between the two phases. KAGRA was expected to join O3, but this initial plan changed due to the outbreak of COVID-19. Instead, KAGRA and GEO 600 [2] operated during an extended observing phase, O3GK, from April 7 to April 21 2020 (Abbott et al. 2022).

The analysis of the O3 data has led to numerous publications. Those include several updates to the GWTC (GW Transient Catalog; Abbott et al. 2021a,b,c) that compiles transient sources analyzed and reported by the combined LIGO-Virgo-KAGRA Collaboration (LVK). The cumulative GWTC catalog currently includes nearly 100 candidate sources (with a probability of astrophysical origin > 50 %), all associated with the coalescence of compact star binaries composed of either neutron stars, black holes, or both.

Following the policy defined in the LIGO Data Management Plan (LIGO Laboratory 2022a) and a Memorandum of Understanding (LIGO Scientific Collaboration and Virgo Collaboration 2019), the O3 data set and associated

* Deceased, December 2021.
† Deceased, March 2022.

[1] Laser Interferometer Gravitational-Wave Observatory

[2] The detector GEO 600 collected data during the O3a and O3b phases of the O3 science run, as indicated in the timeline [3], in the so-called 'Astrowatch' mode. Because of the substantial sensitivity difference between GEO and LIGO or Virgo, the data are not employed in the various analyses and hence are not released publicly. The Astrowatch data can be used in the case of an extraordinary astrophysical event (such as a Galactic core-collapse supernova) during the periods when the other detectors are down.

science products are published through the Gravitational-Wave Open Science Center (GWOSC) at https://gwosc.org [4] allowing the reproducibility of the analyses performed by the LVK and increasing the impact of the data through its wider use. This paper provides a description of the publicly released data (LIGO Scientific Collaboration and Virgo Collaboration 2021a,b; LIGO Scientific Collaboration, Virgo Collaboration and KAGRA Collaboration 2022a) along with additional information on their usage.

To date hundreds of scientific articles have been written using the data available from the GWOSC website (all datasets combined) [5]. These analyses confirm, complement, and extend the results published by the LVK Collaboration. They cover a wide range of topics, including searches for gravitational-wave signals (Olsen et al. 2022; Nitz et al. 2023; Nitz & Wang 2022; Steltner et al. 2023; Whelan et al. 2023), studies of compact binary populations (see e.g., Roulet et al. (2021); Périgois et al. (2023); Callister & Farr (2023), tests of general relativity (see e.g., Capano et al. (2021); Estellés et al. (2022); Wang et al. (2022); Lyu et al. (2022); Capano et al. (2022)), or methodological contributions (see e.g., Davis et al. (2022)), demonstrating the broad impact on the scientific community of the GW data releases.

This paper is organized as follows. Section 2 summarizes the status of the detectors during the observing run O3, together with high-level indicators such as their distance reach and duty cycle of operation. This section also provides insights about how the data are collected and calibrated, about data quality and about simulated signal injections. Section 3 describes the format, content and provenance of the strain data files distributed through the GWOSC, including the nomenclature used for the calibration versions and channel names. Section 4 describes the Event Portal, a searchable GW event database accessible online. Details about the technical validation and review of the data and documentation are given in Section 5. Finally, Section 6 provides some guiding principles to the novice user and suggests software tools that can be used to analyze the data.

2. INSTRUMENTS

The Advanced LIGO (Aasi et al. 2015) and Advanced Virgo (Acernese et al. 2015) detectors are enhanced Michelson interferometers with arm lengths of 4 km and 3 km, respectively. Advanced LIGO comprises two detectors located at two different sites in the US, namely, in Hanford, WA and Livingston LA, while Advanced Virgo has a single site in Cascina, close to Pisa, Italy. The various instrument upgrades realized between the science runs O2 and O3 for the LIGO and Virgo detectors are described in (Buikema et al. 2020; Abbott et al. 2021a,c; Acernese et al. 2022a). They involve many parts of the instruments, including the main laser source and the core optics along with the installation of mitigation systems for a range of technical noises. One of the major novelties in O3 both for LIGO and Virgo is the use of squeezed light sources (see Tse et al. (2019) for LIGO and Acernese et al. (2019) for Virgo), a technique (Schnabel et al. 2010; Barsotti et al. 2019) that significantly reduces quantum noise, thus enhancing the sensitivity at high frequency. Due to the implementation of this technique, the binary neutron star inspiral range (see next section) has increased by 14 %, 12 % and 5-8 % for LIGO Livingston, LIGO Hanford and Virgo, respectively.

GEO 600 (Dooley et al. 2016) is a British–German interferometric GW detector with 600 m arms located near Hannover, Germany. As in LIGO and Virgo, quantum squeezing is used to reduce noise in the output measurement quadrature (Lough et al. 2021). This technique was first demonstrated by GEO 600 (Abadie et al. 2011). KAGRA is an underground laser interferometer with 3-km arms, located underground at the Kamioka Observatory in Gifu Prefecture, Japan. An important feature of its design is the cooling system intended to bring the large mirrors of the interferometer to cryogenic temperature (around 20 K) in order to reduce thermal noise (Akutsu et al. 2016; Chen et al. 2014). During the O3GK run however, the detector was operated at room temperature (Akutsu et al. 2018, 2021).

2.1. *Detectors performance*

A GW detector's performance is often globally characterized by two measures: its duty factor, defined as the fraction of time the detector is recording observational quality data, and its distance reach, conventionally measured as the binary neutron star (BNS) inspiral range (Finn & Chernoff 1993; Chen et al. 2021), the distance to which a BNS inspiral could be detected with signal-to-noise ratio of 8, assuming 1.4 solar mass component objects and averaging over source position and orientation. The choice of this metric is a standard convention. The value of 1.4 solar masses is close to the measured masses of the stars in the Hulse–Taylor binary (Weisberg & Huang 2016) and within the narrow range predicted by stellar evolution for neutron-star masses. The distance reach of the detectors strongly

[4] This website is also accessible at https://gw-openscience.org.

[5] See https://gwosc.org/projects for a list of articles that refer to the data published on the GWOSC website.

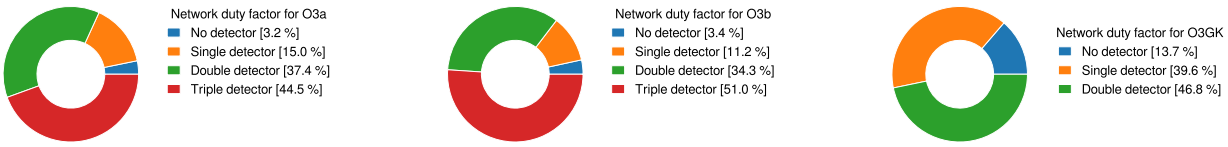

Figure 1. Duty factors for the LIGO and Virgo detector network during O3a (left) and O3b (center) and for the KAGRA and GEO 600 detector network during O3GK (right). These factors measure the fraction of time spent as a function of the number of detectors in operation. The same plots (caveat a difference in the color code) can be found on the GWOSC web summary pages for O3a[6] and O3b[7] and have been produced from Abbott et al. (2022) for O3GK.

depends on the source mass. For example, binary black-hole (BBH) systems can typically be detected at much greater distances, up to several Gpc (e.g., Abbott et al. 2021c, Table IV).

The GWOSC website hosts summary pages for O3a[6] and O3b[7] which describe the LIGO and Virgo operations and sensitivity. The duty factors during O3a are 71% for LIGO Hanford (H1), 76% for LIGO Livingston (L1) and 76% for Virgo (V1). During O3b, the corresponding percentages are 79%, 79% and 76%, respectively. Those translate into the observing factors shown in Fig. 1 that quantify the fraction of observing time spent with one, two or three instruments in operation.

During the O3GK run, the duty factors of KAGRA (K1) and GEO 600 (G1) are 53% and 80% respectively, leading to a coincident observing factor of 47% (Abbott et al. 2022). The lower duty cycle of KAGRA is due to the fact that alignment sensing and control with wavefront sensors was not yet implemented at the time of the run, leading to a higher susceptibility to microseismic ground vibrations.

The median values of the BNS range over the whole observing run are 108 Mpc, 135 Mpc and 45 Mpc for H1, L1 and V1 respectively during O3a, and 115 Mpc, 133 Mpc and 51 Mpc during O3b for the same detectors. The median values of the BNS range over the O3GK period are 0.66 Mpc for KAGRA and 1.06 Mpc for GEO 600. Fig. 2 displays the median BNS range computed over regular intervals (5-minute scale for LIGO and Virgo and 20-minute scale for GEO 600 and KAGRA). The drops that can be observed in both plots are due to transient noise artifacts (discussed in Sec. 2.3) reducing the detector sensitivity temporarily. The BNS range shown in the recent GWTC publications such as Abbott et al. (2021a) (Fig. 3) and Abbott et al. (2021c) (Fig. 3) are averaged over a longer period (1 hour) and are thus less affected by transient noise. The longer gaps in the BNS inspiral range are due to maintenance intervals, instrumental issues, and earthquakes.

2.2. *Calibration*

The GW strain $h(t)$ is obtained and calibrated from variations of the optical power measured at the output port of each detector. The calibration procedure and the corresponding characterization of the systematic and statistical uncertainties are described in Viets et al. (2018); Sun et al. (2020, 2021) for Advanced LIGO and Acernese et al. (2022b) for Advanced Virgo. Calibration is performed in two stages: an initial, online calibration used for low-latency analysis, and a final, offline calibration that applies any needed corrections to the initial result. The offline calibration may correct for computer failures, incomplete modelling of the detectors, or any systematic errors characterized after the observing period. The uncertainties in the calibration procedure for both the magnitude and phase of $h(t)$ as a function of frequency are documented (LIGO Scientific Collaboration & Virgo Collaboration 2021).

The calibration process also includes a noise subtraction step that is based on independent measurements of a number of noise sources by witness sensors, as described in Davis et al. (2019); Vajente et al. (2020a); Mukund et al. (2020); Estevez et al. (2019) and Acernese et al. (2022b). The 60 Hz noise subtraction has increased the range for heavy BBH mergers with a total mass of 70 $M_\odot$ by 25 Mpc for LIGO, while for Virgo, the overall sensitivity was enhanced, resulting in a gain of up to 7 Mpc in the BNS inspiral range. For the last two weeks of O3a, the Virgo data were reprocessed with a new configuration of the noise subtraction (Rolland et al. 2019; Acernese et al. 2022b), resulting in a different calibration being available for this period (see Table 1).

[6] https://gwosc.org/detector_status/O3a

[7] https://gwosc.org/detector_status/O3b

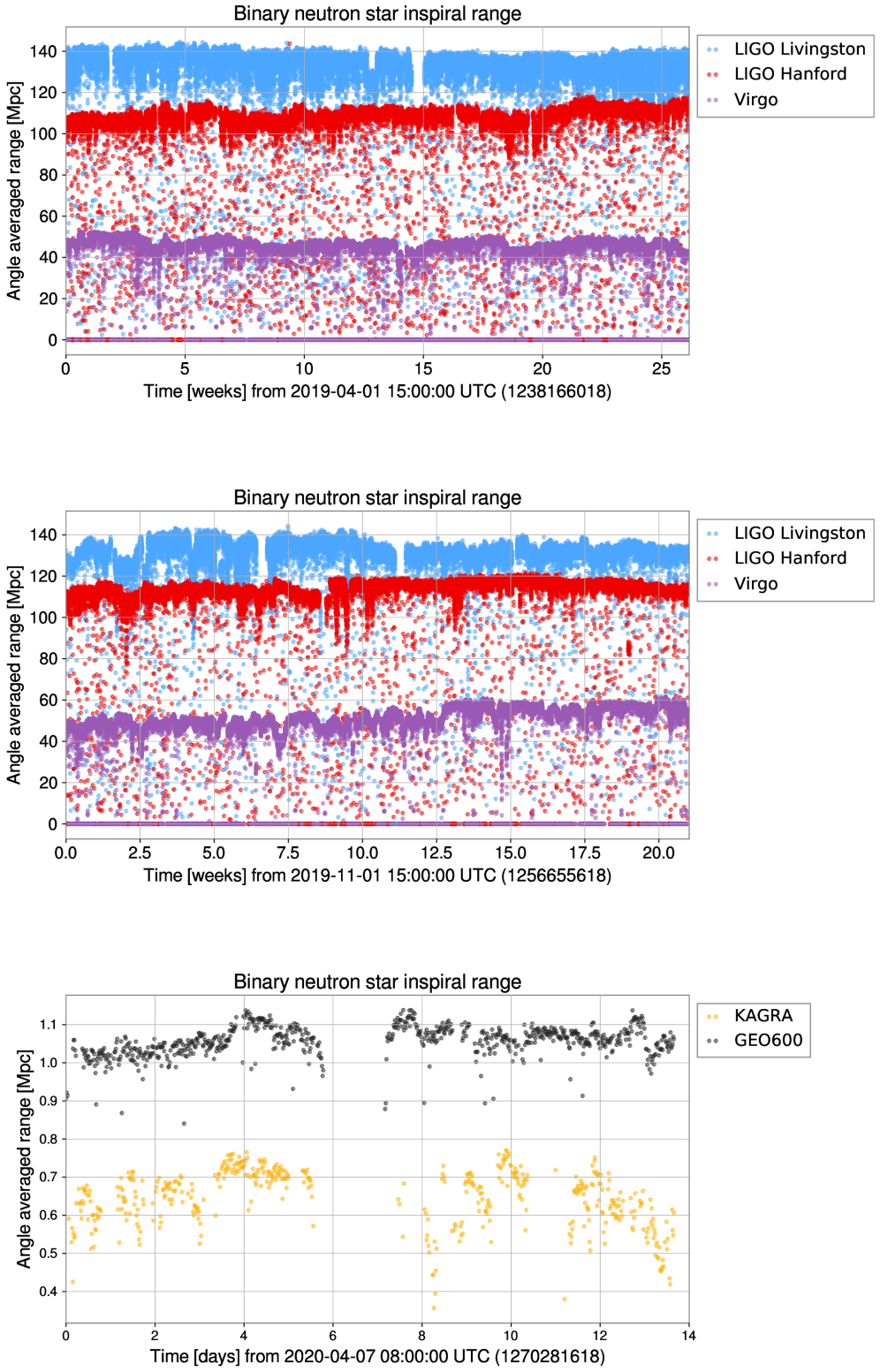

Figure 2. Binary neutron star ranges for O3a (upper plot), O3b (middle plot) with LIGO Hanford (red), LIGO Livingston (blue) and Virgo (purple) and for O3GK (bottom plot) with GEO 600 (black) and KAGRA (yellow). Similar plots (besides style differences) can be found on the GWOSC web pages for O3a [6] and O3b [7] and in Abbott et al. (2022) for O3GK.

GWOSC releases two types of strain data: bulk data spanning an entire observing run, and smaller data snippets around the time of each GW event. Data snippets are based on the calibration version available at the time of publication of the related GW event. Events that appear in multiple publications may have multiple data snippets available, sometimes with different calibration versions. Naturally, the time segments released as data snippets are also available in the bulk data set, but the bulk data of the entire O3a, O3b and O3GK observation runs provided through GWOSC correspond to the final (most up-to-date) calibration. These differences in calibration can lead to discrepancies between the data snippets and the corresponding data in the bulk data release, potentially leading in turn to differences in the source parameter values that can be estimated from the data. However, as discussed in Sec. 3.3, in addition to the main bulk data release, several alternate strain channels with different calibration versions are also made public.

The detector strain $h(t)$ in O3 is calibrated only between 10 Hz and 5000 Hz for Advanced LIGO, between 20 Hz and 2000 Hz for Advanced Virgo, between 30 Hz and 1500 Hz for KAGRA and between 40 Hz and 6000 Hz for GEO 600. Any apparent signal outside these ranges cannot be trusted because it is not a faithful representation of the GW strain at these frequencies. In addition, Advanced Virgo data between 49.5 Hz and 50.5 Hz are characterised by a large increase of calibration errors because of effects related to the mains power lines (Acernese et al. 2022b). Because of this increased systematic error, data in this narrow frequency band were considered to be uninformative for source-parameter estimation (see Appendix E of Abbott et al. (2021c) for relevant methods).

2.3. *Detector noise characterization and data quality*

The data are dominated by instrumental noise that can be well described as Gaussian and stationary over limited time scales and frequency ranges. The data also contain intermittent short-duration noise artifacts, or glitches Glanzer et al. (2023); Acernese et al. (2022c), that contribute to the noise background as well. Any analysis of GW data must account for the presence of these various noise components (see Sec. 6 for more information about using the data). A summary of efforts to characterize data quality in O3 can be seen in Davis et al. (2021a) for Advanced LIGO, Acernese et al. (2022a,c) for Advanced Virgo, and Abe et al. (2022) for KAGRA. The overall quality of data for transient searches is recorded as data quality segments, described in more detail in Sec. 3.2.

2.4. *Signal injections*

Hardware injections are simulated GW signals added by physically displacing the test masses (i.e. the interferometer mirrors) (Biwer et al. 2017). The simulated signal initiates a response that mimics that of a true GW. By looking for discrepancies between the injected and recovered signals, it is possible to characterize the performance of analyses and the coupling of instrumental subsystems to the detectors' output channels.

During the third observing run O3, hardware injections were performed in the Advanced LIGO and Advanced Virgo detectors. The record of all injections is available through GWOSC web pages.[8] This list is provided to prevent potential confusion with an actual astrophysical signal. For Virgo, those injections were removed post-facto when producing the calibrated strain (see Acernese et al. (2022b) for details on this subtraction), so the injection times are not marked in the GWOSC files. On the other hand, in the case of Advanced LIGO the injections are still present in the calibrated data, and their times are marked in the GWOSC files. As further detailed in Sec. 3.2, hardware injections of both short-duration transient signals and long-duration continuous signals were performed. These signals remain in the data so that they may used by analysts for testing purposes. Transient hardware injection were done on a small number of occasions primarily for detector characterization, representing a negligible fraction of the data (less than 300 seconds).

No injections were performed during O3GK.

3. STRAIN DATA

All O3 open data are distributed under the Creative Commons Attribution International Public License 4.0, including strain data from O3a (LIGO Scientific Collaboration and Virgo Collaboration 2021a), O3b (LIGO Scientific Collaboration and Virgo Collaboration 2021b) and O3GK (LIGO Scientific Collaboration, Virgo Collaboration and KAGRA Collaboration 2022a). Small batches of files can be conveniently downloaded from the GWOSC website directly.[9] However, when downloading large amounts of data (such as an entire observing run) the use of the distributed

[8] http://gwosc.org/O3/o3_inj

[9] https://gwosc.org/data

file system `CernVM-FS` (Weitzel et al. 2017) is recommended.[10] Once configured, `CernVM-FS` allows access to all GWOSC data locally on the user's computer.

The O3 calibrated strain data are distributed in files that contain 4096 seconds of data. Published GW signals are also released in separate files containing data snippets of 4096 seconds or 32 seconds, centered on the event's detection time and released under the GWOSC Event Portal.[11] The description of the data records that follows is valid both for single event releases and for bulk data releases.

GWOSC calibrated strain data are repackaged from data stored in the LVK archives. The data source is uniquely identified by a channel name and a frame type (see Table 1). At times when data are unavailable or of quality too poor to be analyzed, the strain values are represented with `NaN`s. Strain data are made available both at the sampling rate of 16384 Hz, and at a downsampled rate of 4096 Hz[12]. Down-sampling is achieved using the standard decimation method implemented in `scipy.signal.decimate`[13] from the Python package SciPy (Virtanen et al. 2020). The highest frequency available is determined by the Nyquist–Shannon sampling theorem (Nyquist 1924), and is equal to half the sampling rate specified in a particular dataset. This is an important consideration to keep in mind when deciding which sample rate to download from GWOSC. Because the anti-aliasing filters used in resampling roll-off at the upper end of the working frequency interval, the valid frequency range is reduced to a bit less than the Nyquist frequency. So, for the 4 kHz data the maximum usable frequency is approximately 1700 Hz. Higher sample rate data will require more hard-drive space to store and longer times to download. The user can decide which dataset meets their needs.

Table 1. The channel names and frame types listed in this table are unique identifiers in the LIGO, Virgo, GEO 600 and KAGRA data archives that allow tracing the provenance of the strain data released on GWOSC. H1 and L1 indicate the two LIGO detectors (Hanford and Livingston respectively), V1 refers to Virgo, G1 refers to GEO 600 and K1 refers to KAGRA. The attribute `CLEAN-SUB60HZ` in H1 and L1 indicates that the noise subtraction procedure described in Vajente et al. (2020b) was used. The attributes `C01`, `V1Online` and `V1O3Repro1A` refer to the calibration version.

Run	Det.	Channel name	Frame type
O3a	H1	`H1:DCS-CALIB_STRAIN_CLEAN-SUB60HZ_C01`	`H1_HOFT_CLEAN_SUB60HZ_C01`
O3a	L1	`L1:DCS-CALIB_STRAIN_CLEAN-SUB60HZ_C01`	`L1_HOFT_CLEAN_SUB60HZ_C01`
O3a	V1	`V1:Hrec_hoft_16384Hz`	`V1Online`
O3a(last two weeks)	V1	`V1:Hrec_hoft_V1O3ARepro1A_16384Hz`	`V1O3Repro1A`
O3b	H1	`H1:DCS-CALIB_STRAIN_CLEAN-SUB60HZ_C01`	`H1_HOFT_CLEAN_SUB60HZ_C01`
O3b	L1	`L1:DCS-CALIB_STRAIN_CLEAN-SUB60HZ_C01`	`L1_HOFT_CLEAN_SUB60HZ_C01`
O3b	V1	`V1:Hrec_hoft_16384Hz`	`V1Online`
O3GK	G1	`G1:DER_DATA_HD_CLEAN`	`G1_RDS_C02_L3`
O3GK	K1	`K1:DAC-STRAIN_C20`	`K1_HOFT_C20`

3.1. *GWOSC file formats*

The GWOSC open data are delivered in two different file formats: `hdf` and `gwf`. The Hierarchical Data Format `hdf` (Koziol & Robinson 2018) is a portable data format readable by many programming languages. The Frame format `gwf` (LIGO Scientific Collaboration and Virgo Collaboration 2009) is a specialized format used by the gravitational wave community. Data associated with GW events are also released as plain text files containing two columns with the global positioning system (GPS) time in the first column and the corresponding strain value in the second column.

For both formats the file naming follows the naming convention,

$$obs\text{—}FrameType\text{—}GPSstart\text{—}duration.extension$$

where *FrameType* for the main O3 data release is

[10] For `CernVM-FS` installation instructions, see https://gwosc.org/cvmfs.

[11] See https://gwosc.org/eventapi.

[12] For simplicity, in the rest of the paper the sampling rates will be indicated in kHz and rounded to the closest integer, i.e. 4 and 16 kHz means 4096 and 16384 Hz, respectively.

[13] This method applies an anti-aliasing filter based on an order-8 Chebychev type I infinite impulse response (IIR) filter (Ellis 2012) before decimation.

*ifo*_GWOSC_*ObservationRun*_*s*KHZ_R*n*

and

- *obs* is the observatory, i.e. the site, so can have values L, H, V, G or K;
- *ifo* is the interferometer and can have values H1, L1, V1, G1 or K1;
- *ObservationRun* encodes the observing run name, so in this case is O3a, O3b, or O3GK;
- *s* is the sampling rate in kHz with either a value 4 or 16 (4096 Hz or 16384 Hz);
- *n* is the version number of the file (typically 1);
- *GPSstart* is the starting time of the data contained in the file, as a 10-digit GPS value (in seconds);
- *duration* is the duration in seconds of the file, typically either 4096 or 32 seconds;
- and *extension* represents the file format and can be `gwf` or `hdf`.

The folders (or groups) included in the `hdf` files are:

- *meta*: metadata of the file containing the following fields:
  - *Description*, e.g. "Strain data time series from LIGO",
  - *DescriptionURL*: URL of the GWOSC website,
  - *Detector*, e.g. L1, and *Observatory*, e.g. L,[14]
  - *Duration*, *GPSstart*, *UTCstart*: duration and starting time (using GPS and UTC standards, respectively) of the segment of data contained in a file.
  - *StrainChannel*: channel name used in the LVK archives
  - *FrameType*: frame type used in the LVK archives
- *strain*: array of $h(t)$, sampled at 4 or 16 kHz depending on the file. For the times when the detector is not in science mode or the data does not meet the minimum required data quality conditions (see next section), the strain values are set to `NaN`s. The strain $h(t)$ is a function of time, so it is accompanied by the attributes *Xstart* and *Xspacing* defining the starting GPS time of the data contained in the array and the corresponding distance in time between the points of the array.
- *quality*: this folder contains two sub-folders, one for data quality and the other for injections, each including a bitmask to indicate at each second the status of the data quality or the injections and the description of each bit of the mask (see Section 3.2 for details).

The `gwf` files have a similar content but with a different structure. They contain 3 channels, one for the strain data, one for the data quality and one for the injections. The channel names are described in Table 2. The original files produced internally, whose channel names are listed in Table 1, contain only the strain channel, while the GWOSC files conveniently combine the strain data with the data quality and injection information in the same file.

Table 2. Channel names of the GWOSC frame files (format `gwf`). In this nomenclature, *ifo* is a place holder for the interferometer name, i.e. H1, L1, V1, G1 or K1, and $s = 4$ or 16 kHz denotes the sampling rate. The `R1` sub-string represents the revision number of the channel name so it will become `R2` in case there is a second (revised) release, and so on.

	Channel name
Strain	*ifo*:GWOSC-*s*KHZ_R1_STRAIN
Data quality mask	*ifo*:GWOSC-*s*KHZ_R1_DQMASK
Injections mask	*ifo*:GWOSC-*s*KHZ_R1_INJMASK

[14] The observatory refers to the site and it is indicated by one letter, like L for Livingston. The addition of a number after the letter to indicate the detector, e.g. L1, could be useful if multiple detectors are installed in the same site, as was the case for Initial LIGO (Abbott et al. 2009).

3.2. *Data quality and injections in GWOSC files*

The LVK performs several types of searches are on LIGO, Virgo, GEO 600, and KAGRA data. Those searches are divided into four families named after the types of signals they target: Compact binary coalescences (`CBC`), GW bursts (`BURST`), continuous waves (`CW`) and stochastic backgrounds (`STOCH`). As each type of search has a unique sensitivity to instrumental artifacts, a detailed characterization of detector noise and data quality is essential to eliminate spurious signals of terrestrial origin found by the searches. LIGO, Virgo, GEO 600 and KAGRA have dedicated teams responsible for detector characterization and data quality, as described in Davis et al. (2021a); Acernese et al. (2022a); Abbott et al. (2022), and Abe et al. (2022).

`CBC` analyses (Sachdev et al. 2019; Aubin et al. 2021; Davies et al. 2020) seek signals from merging neutron stars and black holes by filtering the data with waveform templates. `BURST` analyses (Klimenko et al. 2016; Cornish et al. 2021) search for generic GW transients with minimal assumptions on the source or signal morphology by identifying excess power in the time-frequency representation of the GW strain data. `CW` searches (Astone et al. 2014; Krishnan et al. 2004; Aasi et al. 2014) look for long-duration, continuous, periodic GW signals from asymmetries of rapidly spinning neutron stars. `STOCH` searches (Allen & Romano 1999; Abbott et al. 2021e,f) target the stochastic GW background signal which is formed by the superposition of and unresolved sources from various stages of the evolution of the universe.

Because of fundamental differences in the search methodologies, certain noise types are relevant to specific searches (Davis et al. 2021b). `CBC` and `BURST` searches look for short, transient signals, with durations from less than a second to several tens of seconds (see e.g., Sathyaprakash & Schutz (2009)). Data quality information for these searches is recorded as sets of time intervals when data are relatively free of corruption, known as segment lists, described in Davis et al. (2021b). This information is provided inside the GWOSC files for the two GW transient searches `CBC` and `BURST`. The data quality information most relevant for `CW` and `STOCH` searches is in the frequency domain and it is provided as lists of instrumental lines in separate files, available for download on GWOSC[15].

Data quality and signal injection information for a given GPS second is indicated by bitmasks with a 1-Hz sampling rate. The bit meanings are given in Tables 3 and 4 for the data quality and injections, respectively. To describe data quality, different *categories* are defined. For each category, the corresponding bit in the bitmask shown in Table 3 has a value of 1 (good data) if in that second of time the requirements of the category are fulfilled, otherwise 0 (bad data).

Table 3. Data quality bitmasks description. For O3, the `CBC_CAT1` and `BURST_CAT1` segment lists are equivalent (see the definition of `CAT1` in the text). Note that any data that are not present are replaced by `NaN` values in the corresponding strain time series. In each bit mask, a value of 1 corresponds to the data quality check passing (good data), and a zero means the check has failed (bad data). The `CBC_CAT3` and `BURST_CAT3` are equivalent to `CBC_CAT2` and `BURST_CAT2` in O3.

Bit	Short name	Description
0	`DATA`	Data present
1	`CBC_CAT1`	Pass `CAT1` test
2	`CBC_CAT2`	Pass `CAT1` and `CAT2` test for `CBC` searches
3	`CBC_CAT3`	Pass `CAT1` and `CAT2` and `CAT3` test for `CBC` searches
4	`BURST_CAT1`	Pass `CAT1` test
5	`BURST_CAT2`	Pass `CAT1` and `CAT2` test for `BURST` searches
6	`BURST_CAT3`	Pass `CAT1` and `CAT2` and `CAT3` test for `BURST` searches

The meaning of the categories is described in Davis et al. (2021a) and Acernese et al. (2022c). The specific categories are described in Section 5.2 of Davis et al. (2021a) and in Sections 4 and 6.4.1 of Acernese et al. (2022c). The complete list of channels used to construct the segment lists are available on the GWOSC website [16]. Here, we provide a brief summary of each category:

[15] See https://gwosc.org/O3/o3speclines for L1, H1 and V1, https://gwosc.org/O3/O3GKspeclines for K1 and https://gwosc.org/O3/O3GK_GEO_speclines for G1.

[16] https://gwosc.org/O3/auxiliary

Table 4. Meaning of the injection bits. A value of 1 indicates `TRUE` (no injection), while a value of 0 is `FALSE` (injection is present).

Bit	Short name	Description
0	`NO_CBC_HW_INJ`	No `CBC` injections
1	`NO_BURST_HW_INJ`	No burst injections
2	`NO_DETCHAR_HW_INJ`	No detector characterization injections
3	`NO_CW_HW_INJ`	No continuous wave injections
4	`NO_STOCH_HW_INJ`	No stochastic injections

`DATA`: Failing this level indicates that strain data are not publicly available at this time because the instruments were not operating in nominal conditions. For O3, this is equivalent to failing Category 1 criteria, defined below. For intervals of bad or absent data, `NaN`s have been inserted in the corresponding strain data array.

`CAT1`: (Category 1) Failing a data quality check at this category indicates a critical issue with a key detector component not operating in its nominal configuration. GWOSC data during times that fail `CAT1` criteria are replaced by `NaN` values in the strain time series. For O3, `CBC_CAT1`, `BURST_CAT1`, and `DATA` lead to identical segment lists. Applying `CAT1` flags removes around 0.3%, $\sim 1\%$ and 0.2% of observing time for LIGO Hanford, LIGO Livingston, and Virgo respectively (Davis et al. 2021a; Acernese et al. 2022a).

`CAT2`: (Category 2) Failing a data quality check at this category indicates times when excess noise is present in a sensor with an understood physical coupling to the strain channel (LIGO Scientific Collaboration and Virgo Collaboration 2016). The fraction of time removed by this category is less than 1% of the data, and is detailed in Table 6.

`CAT3`: (Category 3) Failing a data quality check at this category indicates times when there is statistical coupling between a sensor/auxiliary channel and the strain channel which is not fully understood. This category was not used in O3 LVK searches, although it was used in previous observing runs (Abbott et al. 2021d).

Table 5. Total time satisfying the data quality criteria for each `SEARCH` type (= `CBC` or `BURST`) and each `CATEGORY` (= `CAT1`, `CAT2` or `CAT3`) spanning the full `DURATION` of each observing `RUN` (= O3a, O3b or O3GK) and each `DETECTOR` (= H1, L1, V1, G1 or K1). `DURATION` includes all time in seconds between the official start and end of each `RUN`, including times when the instruments are not collecting data for astrophysical analysis. When the criteria for a given flag is satisfied, the corresponding bit will have the value 1 (good data by these criteria); otherwise, it will have the value 0 (bad data). The data in the table can be retrieved at https://gwosc.org/timeline/show/[RUN]_16KHZ_R1/[DETECTOR]_[SEARCH]_[CATEGORY].

Data Quality Flags (Total time in seconds)									
RUN	DURATION	DETECTOR	DATA	CBC_CAT1	CBC_CAT2	CBC_CAT3	BURST_CAT1	BURST_CAT2	BURST_CAT3
O3a	15811200	H1	11218675	11218675	11177046	11177046	11218675	11125849	11125849
		L1	11956179	11956179	11943913	11943913	11956179	11879365	11879365
		V1	12038929	12038929	12038929	12038929	12038929	12038929	12038929
O3b	12708000	H1	9967195	9967195	9964945	9964945	9967195	9915276	9915276
		L1	9810816	9810816	9782946	9782946	9810816	9760960	9760960
		V1	9591207	9591207	9591207	9591207	9591207	9591207	9591207
O3GK	1180800	G1	940133	940133	940133	940133	940133	940133	940133
		K1	628055	628055	628055	628055	628055	628055	628055

Data quality categories are cascading: a time which fails a given category automatically fails all higher categories. Since `CAT3` flags were not used in O3, the `CAT3` segment lists are identical to the corresponding `CAT2` lists. However, the different analysis groups qualify the data independently: failing `BURST_CAT2` does not necessarily imply failing `CBC_CAT2`. See Table 5 for the amount of time associated with each category.

Table 6. Fraction of observing time removed by applying CAT2 vetoes. The percentages represent the amount of time in the DATA segment list relative to the total duration of observing time. CAT2 vetoes were not used for Virgo, KAGRA, or GEO 600.

Detector	O3a		O3b	
	CBC	BURST	CBC	BURST
H1	0.37%	0.83%	0.02%	0.52%
L1	0.01%	0.64%	0.28%	0.51%

Simulated signals added to the detectors for testing and calibration are referred to as *hardware injections*. GWOSC data releases provide a time series with each one second sample representing a bit mask vector of the state of the injection at that time. The injections are categorized according to the type of injected signal relevant to each astrophysical search. There are also injections used for detector characterization (DETCHAR). The injection bitmask marks the injection-free times. The bit corresponding to a given type of injection is defined in Table 4. A bit is set to 1 if there is no injection, otherwise it is set to 0. The full details of the complete set of hardware injections for O3 can be found at https://gwosc.org/O3/o3_inj.

There were no CBC injections during O3. As documented in the above page of the GWOSC website, the timelines of H1 and L1 contain a segment erroneously marked as associated with a CBC injection. Those segments are between GPS 1251662270 (2019-09-04T19:57:32 UTC) and GPS 1251662279 (2019-09-04T19:57:41 UTC) and between GPS 1251585495 (2019-09-04T00:37:57 UTC) and GPS 1251585503 (2019-09-04T00:38:05 UTC) for H1 and L1 respectively.

No injections of BURST signals were performed during O3a and O3b.

Some signal injections of the DETCHAR type were injected during O3a and O3b for both H1 and L1, while there were none for Virgo. The waveform model used for those injections is $h(t) = a\ e^{-(t-t_0)^2/\tau^2} \sin\left[2\pi f(t-t_0) - \phi\right]$, where t_0 is the time of the injection. The signal parameters τ, ϕ and f were randomly chosen and are documented in separate databases for H1[17] and for L1[18].

Four STOCH signals were injected during O3. These hardware injections consisted of a simulated stochastic gravitational-wave background of 13 minutes long duration and were generated using the NAP package (Acernese et al. 2005) and rescaled to have an amplitude of $\Omega_0 = 2.0 \times 10^{-5}$ with the default Hubble constant value $H_0 = 100$ km s^{-1} Mpc^{-1}. Two of these injections were added only in H1 starting at GPS 1249200018 (2019-08-07T08:00:00 UTC) and GPS 1258273818 (2019-11-20T08:30:00). The other two injections were performed coherently at L1 and H1 during O3b starting at GPS 1258345818 (2019-11-21T04:30:00) and GPS 1258353018 (2019-11-21T06:30:00). The detectors were in observing mode for all of these stochastic injections.

CW injections were performed in H1 and L1 during both O3a and O3b, using a set of pulsar parameters provided on the GWOSC website[19]. CW hardware injections are extremely helpful for a variety of reasons. Critically, they allow an end-to-end test of a signal that is physically present in the instrument that goes through the control loops, calibration, cleaning, intermediate data products and analysis. The output of the analysis is compared with the expected waveform. Any inconsistency could point to a problem somewhere that could be further investigated. In contrast, a software injection can only be added after the calibration step, meaning only half the pathway from physical signal to analysis result would be tested. As a secondary benefit, the hardware injections also allow a direct comparison of analysis methods and results on a consistent set of signals without having to coordinate different software injection campaigns where different choices can yield different answers.

The CW injections are always present except during defined intervals for O3a[20] and O3b[21]. No CW injections were performed in V1 during O3a, but there were CW injections in V1 during O3b between GPS 1263945616 (2020-01-24 23:59:58 UTC) and GPS 1266019220 (2020-02-18 00:00:02 UTC). The injected signal was removed a posteriori in the strain data as described in Acernese et al. (2022b). A residual signal after removal may still be present with an amplitude between 20 and 100 times lower than that of the injection. The residual amplitude is smaller than or at most the same order as the calibration uncertainty.

[17] See https://gwosc.org/static/injections/o3a/H1_detchar_inj.txt for O3a and https://gwosc.org/static/injections/O3b/inj_o3b_H1.txt for O3b.

[18] See https://gwosc.org/static/injections/o3a/L1_detchar_inj.txt for O3a and https://gwosc.org/static/injections/O3b/inj_o3b_L1.txt for O3b.

[19] https://gwosc.org/O3/O3April1_injection_parameters

[20] https://gwosc.org/timeline/show/O3a_16KHZ_R1/H1_NO_CW_HW_INJ*H1_DATA*L1_NO_CW_HW_INJ*L1_DATA/1238166018/15811200

[21] https://gwosc.org/timeline/show/O3b_16KHZ_R1/H1_NO_CW_HW_INJ*H1_DATA*L1_NO_CW_HW_INJ*L1_DATA/1256655618/12708000

No signal hardware injections of any type were performed during O3GK.

3.3. *Alternate versions of the strain data*

Table 7. Names of alternate strain channels in the O3 data release. *ifo* is a place holder for the name of the LIGO interferometer, i.e. H1 or L1.

Channel name	Description
ifo:DCS-CALIB_STRAIN_C01_AR	LIGO calibrated strain, offline calibration
ifo:DCS-CALIB_STRAIN_CLEAN_C01_AR	LIGO calibrated strain, after applying linear noise subtraction
ifo:DCS-CALIB_STRAIN_CLEAN_SUB60HZ_C01_AR	LIGO calibrated strain, after applying both linear and non-linear noise subtraction. This is the recommended channel (main release)
V1:Hrec_hoft_16384Hz_AR	Virgo calibrated strain for most of O3a and O3b (main release)
V1:Hrec_hoft_V1O3ARepro1A_16384Hz_AR	Virgo calibrated strain for the last two weeks of Sep 2019, near the end of O3a with an enhanced noise subtraction (main release)

In addition to the main strain data release described above, the O3 data release includes several alternate strain channels, as described at https://gwosc.org/O3/O3alt. This alternate data release is available via both `CernVM-FS` or streaming via a network data server (NDS2) (Zweizig et al. 2021). The alternate strain channels reflect different choices for how aggressively to apply noise subtraction strategies to remove different sources of contamination. Some LVK analyses used different versions of the strain channels. The alternate strain channel release was designed to reflect the internal formatting used by the LVK as much as possible. In particular, the release uses only the `GWF` file format, does not include any `NaN` values, and does not include any data quality information. The channels found in the alternate calibration release are described in Table 7. For LIGO, the alternate channel release includes all times covered by the main strain dataset, but also includes times in observing mode that fail the `CAT_1` data quality flag. For Virgo, the alternate channel release covers the same times as the main strain dataset.

4. ONLINE EVENT CATALOGS

Ninety-three GW transient events or notable candidates were discovered based on the LVK's analyses of the O3 data (Abbott et al. 2021a,b,c). Data associated with these signals are available online through the GWOSC Event Portal[22], along with other scientific products. For all events in the Event Portal, snippets of strain data are released in the form of a segment of 4096 seconds around the time of the event. The data snippets are made available no later than when the event discovery becomes public in a refereed, scientific journal. In addition, the Event Portal includes a concise summary of the source properties (i.e., parameters of the compact star binaries associated with each of the detected signals), links to a number of science products (posterior samples), links to any associated low-latency alerts, and a documentation page for each release containing publication information. The list of O3 event data releases is as follows:

`O3_Discovery_Papers`: Notable events first published individually (Abbott et al. 2020b,d,e,f, 2021g). Associated data releases may contain preliminary versions of data quality segments and calibration

`O3_IMBH_marginal`: Marginal candidates associated with the search for Intermediate Mass Black Hole (IMBH) binary mergers

`GWTC-2`: Confident events from the O3a observation run (first search)

`GWTC-2.1-confident`: Confident events from the O3a observation run (updated search)

[22] https://gwosc.org/eventapi

`GWTC-2.1-marginal`: Marginal candidates from the O3a observation run (updated search)

`GWTC-2.1-auxiliary`: Candidates from GWTC-2 which, based on the updated analysis presented in the GWTC-2.1 catalog paper, do not satisfy the criteria for inclusion in the GWTC-2.1-confident or GWTC-2.1-marginal releases

`GWTC-3-confident`: Confident events from the O3b observing run

`GWTC-3-marginal`: Marginal candidates from the O3b observing run

Some events are listed in the database with multiple versions, typically corresponding to the event's inclusion in multiple releases. The cumulative `GWTC` catalog includes all confident GW events published by the LVK collaboration, and currently includes 93 events. Events in the `GWTC-2.1-confident` and `GWTC-3-confident` releases all have a probability of astrophysical origin greater than 0.5 [23] in at least one of the search pipelines, and are included in the cumulative `GWTC`.

The online catalogs are searchable via a web user interface. The Event Portal database can be queried based on specific source properties, namely the primary mass, secondary mass, total mass, chirp mass, final mass (of the merger remnant), luminosity distance, redshift, effective inspiral spin, or other properties associated with the observed signal, such as UTC or GPS event time, detector frame chirp mass, network SNR, false alarm rate and the posterior probability of astrophysical origin. The events can also be selected by identification such as partial event name, release catalog or group of catalogs. The output format can be one of the following: HTML, JSON, CSV or plain ASCII text.

To ease the analysis of multiple events, the catalogs can be queried programmatically with scripts using the REST API that returns all catalog lists in a JSON format. Catalogs can be queried with a `GET` request. As an example, to request all merger events for which the primary mass is less than $3M_\odot$, the URL for the `GET` request would be https://gwosc.org/eventapi/html/query/show?max-mass-1-source=3. A detailed explanation of the query API nodes can be found on the GWOSC website[24].

4.1. *Parameter estimation and other science data products*

In addition to the information provided by GWOSC, complementary data about various aspects of the GWTC catalog production are available on the Zenodo open repository, see LIGO Scientific Collaboration and Virgo Collaboration (2021c,d, 2022a) for GWTC-2 and GWTC-2.1 and LIGO Scientific Collaboration, Virgo Collaboration and KAGRA Collaboration (2021a,b, 2023a, 2021c) for GWTC-3. They are linked from the documentation in GWOSC [25]. Those include lists of candidate events, the description of the search pipeline sensitivity and data quality products.

The additional data release also include posterior samples from Bayesian inference analyses, see LIGO Scientific Collaboration and Virgo Collaboration (2022b) for GWTC-2.1 and LIGO Scientific Collaboration, Virgo Collaboration and KAGRA Collaboration (2021d) for GWTC-3. For convenience, those data are directly linked from the single event page of the online catalog. They can also be programmatically accessed through the JSON API as downloadable links to the files on Zenodo.

The parameter names in the posterior samples follow a standard nomenclature[26] (Hoy & Raymond 2021). Parameter estimates may change with the different versions of the event or catalog release. The users should refer to the release pages on Zenodo (LIGO Scientific Collaboration and Virgo Collaboration 2022b; LIGO Scientific Collaboration, Virgo Collaboration and KAGRA Collaboration 2021d) and their associated publications (Abbott et al. 2021b,c) to obtain the full details about the configuration and assumptions made by the different analyses that are denoted by set of version numbers for each event (depending on the number of releases in which that event appears). For each detected source the Event Portal displays the 90% credible intervals for a selection of parameters that reflect the values given in the relevant publication. Those credible intervals are computed from the posterior samples.

In some cases, the parameter estimation made use of "glitch-subtracted frames", where a model for an apparent instrumental artifact was computed and subtracted from the strain data. These glitch-subtracted frames are made available via Zenodo (LIGO Scientific Collaboration and Virgo Collaboration 2022c; LIGO Scientific Collaboration, Virgo Collaboration and KAGRA Collaboration 2021e) [27].

[23] See Abbott et al. (2021c), App. D. 7 for a definition and details about its estimation.

[24] https://gwosc.org/apidocs

[25] See https://gwosc.org/GWTC-2, https://gwosc.org/GWTC-2.1 and https://gwosc.org/GWTC-3.

[26] See https://lscsoft.docs.ligo.org/pesummary/stable_docs/gw/parameters.html for a definition.

[27] See also https://dcc.ligo.org/LIGO-T2000470/public.

For GWTC-3, there are other data releases associated with studies of compact binary populations or cosmology (LIGO Scientific Collaboration, Virgo Collaboration and KAGRA Collaboration 2023b, 2021f)

4.2. *Low-latency alerts*

During O3, public alerts were communicated with low latency to report the occurence of a notable trigger detected in the data[28]. The alerts are sent with a latency of few minutes after detection. They include a number of preliminary parameter estimations that are useful for the localization of the source through a probability skymap. This information can be used by other, non-GW, instruments to search for potential electromagnetic counterparts in follow-up observations. The complete list of alerts sent during O3 can be found publicly in the GraceDB website[29] and, as described below, in GWOSC.

The Event Portal references the GraceDB entry for the original trigger alert of the event. Links to GraceDB entries are available through the GWOSC web interface and the JSON API. Events first detected offline do not trigger low-latency alerts and thus lack a GraceDB entry.

5. TECHNICAL VALIDATION

The O3 GWOSC data release is repackaged for the broader user community beginning with the internal strain data products used for data analysis by the LIGO, Virgo, and KAGRA Collaborations for publication purposes. The repackaging produces new GWOSC `gwf` and `hdf5` files containing the previously discussed strain, data quality and hardware injection information for each detector. The repackaging allows us to add data quality segments, remove times outside of observing mode, and simplify the channel names. In addition, versions of these GWOSC files at a reduced sampling rate of 4096 Hz for the strain channel of each detector are also produced. All data for the release are carefully reviewed by the internal GWOSC team and then reviewed by an independent review team made up of members from the LIGO, Virgo, and KAGRA Collaborations. This review process checks that:

- the strain vectors at the maximum sample rate (16 kHz) in the GWOSC `hdf` and `gwf` files are identical to machine precision to the corresponding strain vectors of the LVK main archives;
- the strain vectors after resampling at 4 kHz do not have numerical artifacts that may arise from the resampling technique;
- the data quality and injection information located in either the GWOSC `hdf` and `gwf` files or the online *Timeline* tool described in detail in Section 6, agree with all available records.
- the documentation associated with the O3 data products found online is correct and contains comprehensive information for the broader user community.

The data files and accompanying documentation are released to the public on the GWOSC website once all checks have passed at the designated date and time agreed to by the LIGO, Virgo and KAGRA Collaborations.

6. USAGE NOTES

6.1. *Salient features of GW data*

Working with GW data requires an awareness of the presence of noise in the data. An overview of LIGO/Virgo detector noise and some applicable signal processing methods are described in Abbott et al. (2020c); see also above in Sec. 3.2 and 2.3 for a brief introduction to various classes of detector noise. In addition, as mentioned previously, the data are only valid within a fixed frequency range due to the limits of calibration (Sec. 2.2) as well as due to artifacts from the down-sampling process (Sec. 3). All of these complications need to be considered when searching for astrophysical signals.

6.2. *List of observing segments*

Segment lists describe times when GW detectors are collecting data and are operating in a normal condition, as described in Section 3.2. The GWOSC website provides an online app called `Timeline` to discover, plot, and download

[28] See https://emfollow.docs.ligo.org/userguide for more details. This userguide is a living document that is being updated in preparation for the upcoming science run O4. Therefore, the informations in this guide may not be necessarily relevant for O3 data.

[29] https://gracedb.ligo.org/superevents/public/O3

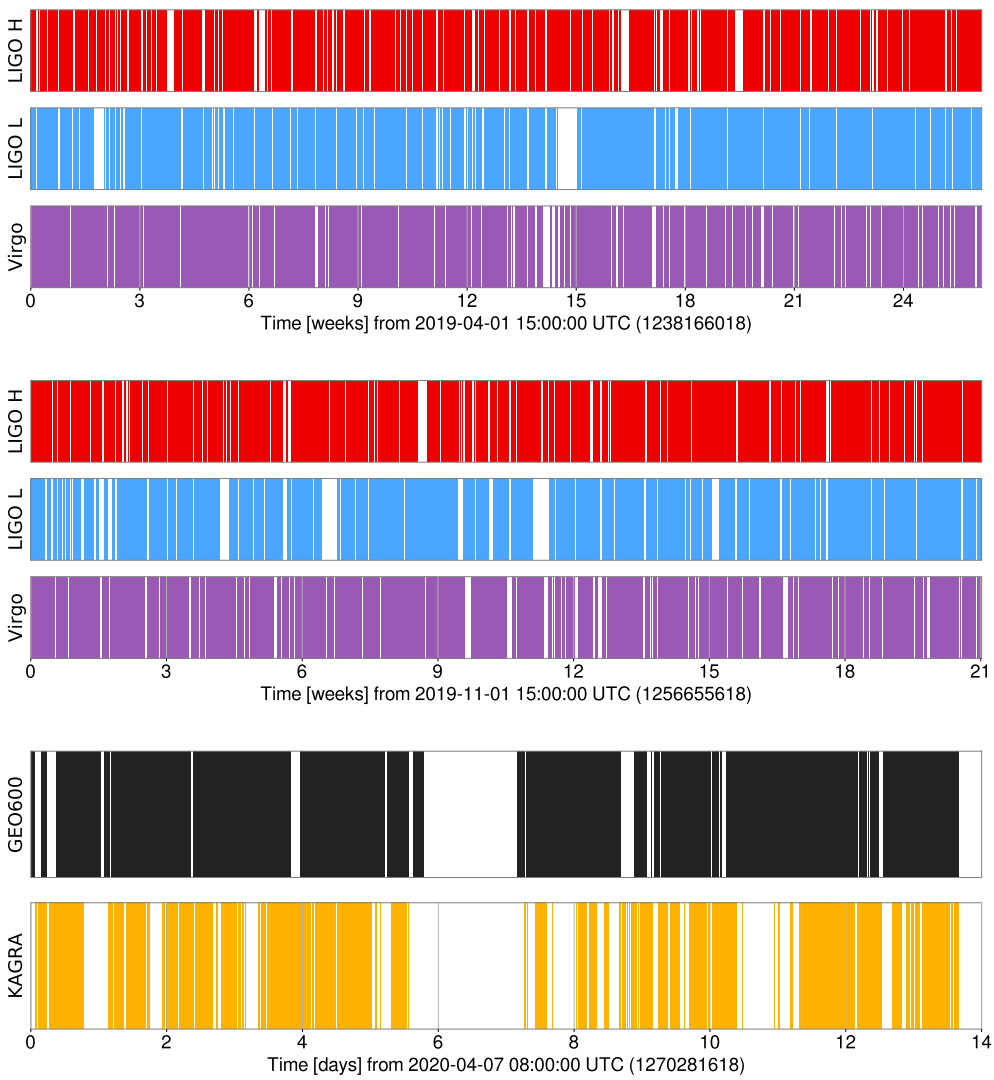

Figure 3. Timelines for the full O3a (top) and O3b (middle) and O3GK (bottom) observing runs based on the data quality bitmask `CBC_CAT1` for each detector (see Tab. 3). Colored bars represent times when data are available, and white areas show times when data are not available. Similar plots can be generated from the GWOSC web pages[30].

segment lists[30]. The Timeline query page allows users to select observing runs from a drop-down menu, and then view the names of segment lists associated with the selected run. Segment lists may be downloaded as ASCII text files or in a JSON format. Alternatively, segment lists may be displayed in an interactive plot, as seen in Fig. 3. To explore times within a run, a visitor can use the mouse to scroll and zoom on the Timeline plots. Hovering the mouse over a segment displays a tool-tip with the exact start and stop time, in both GPS and UTC time.

6.3. *Software and Support*

The GWOSC website provides a number of resources for helping investigators learn to work with GW data, including:

- **Software libraries**[31]: A number of software packages developed for GW analysis are open source. The GWOSC website provides a suggested list of packages, many of which were created by members of the LIGO, Virgo, and KAGRA collaborations. This list includes GstLAL Sachdev et al. (2019), MBTA Aubin et al. (2021), PyCBC

[30] See https://gwosc.org/timeline.

[31] https://gwosc.org/software

Davies et al. (2020), cWB Klimenko et al. (2016), BayesWave Cornish et al. (2021), GWpy Macleod et al. (2021c) and Bilby Ashton et al. (2019). Links to source code and documentation are provided for each package.

- **Tutorials**[32]: GWOSC provides tutorials to demonstrate the basics of GW data analysis. Most tutorials are in `Python`, and provided in notebooks that can be run in the cloud to avoid the necessity for the user to install software.

- **Workshops and online course**[33]: Annual Open Data Workshops provide a complete course in working with GW data, including lectures, software tutorials, and challenge problems. Materials from past workshops are available as a free online course; students can enroll at any time. Future workshops will be posted on the GWOSC website, and are open to any interested participants.

- **Discussion forum**[34]: A public discussion forum for GW topics provides space to ask for help with GW data analysis, discuss LVK papers, post questions about GW science, and connect with other researchers in the field.

7. SUMMARY

The O3 data set described in this paper represents the most sensitive gravitational-wave observations to date. The data contain over 80 compact object merger signals, as described in a number of catalog releases, including GWTC-2 (Abbott et al. 2021a), GWTC-2.1 (Abbott et al. 2021b) and GWTC-3 (Abbott et al. 2021c). O3 includes three main phases: O3a, O3b, and O3GK. O3a and O3b are both joint runs of LIGO and Virgo, while the O3GK run involved KAGRA and GEO 600. Data and documentation for all O3 data are available from the GWOSC website.

Looking ahead, LIGO, Virgo, and KAGRA are planning an O4 run, scheduled to begin in 2023, with improved sensitivity. Data from events discovered in O4 will be released as the events are published, and release of the next large strain data sets are planned for 2025 (LIGO Laboratory 2022b). This will be followed by the O5 observing run, anticipated to be the first extended observing run with a span of over two years (LIGO Scientific Collaboration, Virgo Collaboration and KAGRA Collaboration 2022b). Planned instrument upgrades should increase the sensitivity of the network and thus extend the volume of space over which signals may be observed, so that future data sets will include more frequent detections and a corresponding expanded depth of science in this rapidly evolving field.

[32] https://gwosc.org/tutorials
[33] https://gwosc.org/workshops
[34] https://ask.igwn.org

ACKNOWLEDGEMENTS

Calibration of the LIGO strain data was performed with GstLAL-based calibration software pipeline (Viets et al. 2018). Calibration of the Virgo strain data was performed with C-based software (Acernese et al. 2022b). Data-quality products and event-validation results were computed using the DMT (John Zweizig 2006), DQR (LIGO Scientific Collaboration and Virgo Collaboration 2018), DQSEGDB (Fisher et al. 2021), gwdetchar (Urban et al. 2021), hveto (Smith et al. 2011), iDQ (Essick et al. 2020) and Omicron (Robinet et al. 2020) software packages and contributing software tools. Analyses relied upon the LALSuite software library (LIGO Scientific Collaboration 2018). PESummary was used to post-process and collate parameter-estimation results (Hoy & Raymond 2021). For an exhaustive list of the softwares used for searching the GW signals and characterizing their source, see (Abbott et al. 2021c). Plots were prepared with Matplotlib (Hunter 2007), seaborn (Waskom 2021) GWSumm (Macleod et al. 2021a) and GWpy (Macleod et al. 2021b). NumPy (Harris et al. 2020) and SciPy (Virtanen et al. 2020) were used in the preparation of the manuscript.

This material is based upon work supported by NSF's LIGO Laboratory which is a major facility fully funded by the National Science Foundation. The authors also gratefully acknowledge the support of the Science and Technology Facilities Council (STFC) of the United Kingdom, the Max-Planck-Society (MPS), and the State of Niedersachsen/Germany for support of the construction of Advanced LIGO and construction and operation of the GEO 600 detector. Additional support for Advanced LIGO was provided by the Australian Research Council. The authors gratefully acknowledge the Italian Istituto Nazionale di Fisica Nucleare (INFN), the French Centre National de la Recherche Scientifique (CNRS) and the Netherlands Organization for Scientific Research (NWO), for the construction and operation of the Virgo detector and the creation and support of the EGO consortium. The authors also gratefully acknowledge research support from these agencies as well as by the Council of Scientific and Industrial Research of India, the Department of Science and Technology, India, the Science & Engineering Research Board (SERB), India, the Ministry of Human Resource Development, India, the Spanish Agencia Estatal de Investigación (AEI), the Spanish Ministerio de Ciencia e Innovación and Ministerio de Universidades, the Conselleria de Fons Europeus, Universitat i Cultura and the Direcció General de Política Universitaria i Recerca del Govern de les Illes Balears, the Conselleria d'Innovació, Universitats, Ciència i Societat Digital de la Generalitat Valenciana and the CERCA Programme Generalitat de Catalunya, Spain, the National Science Centre of Poland and the European Union – European Regional Development Fund; Foundation for Polish Science (FNP), the Swiss National Science Foundation (SNSF), the Russian Foundation for Basic Research, the Russian Science Foundation, the European Commission, the European Social Funds (ESF), the European Regional Development Funds (ERDF), the Royal Society, the Scottish Funding Council, the Scottish Universities Physics Alliance, the Hungarian Scientific Research Fund (OTKA), the French Lyon Institute of Origins (LIO), the Belgian Fonds de la Recherche Scientifique (FRS-FNRS), Actions de Recherche Concertées (ARC) and Fonds Wetenschappelijk Onderzoek – Vlaanderen (FWO), Belgium, the Paris Île-de-France Region, the National Research, Development and Innovation Office Hungary (NKFIH), the National Research Foundation of Korea, the Natural Science and Engineering Research Council Canada, Canadian Foundation for Innovation (CFI), the Brazilian Ministry of Science, Technology, and Innovations, the International Center for Theoretical Physics South American Institute for Fundamental Research (ICTP-SAIFR), the Research Grants Council of Hong Kong, the National Natural Science Foundation of China (NSFC), the Leverhulme Trust, the Research Corporation, the Ministry of Science and Technology (MOST), Taiwan, the United States Department of Energy, and the Kavli Foundation. The authors gratefully acknowledge the support of the NSF, STFC, INFN and CNRS for provision of computational resources.

This work was supported by MEXT, JSPS Leading-edge Research Infrastructure Program, JSPS Grant-in-Aid for Specially Promoted Research 26000005, JSPS Grant-inAid for Scientific Research on Innovative Areas 2905: JP17H06358, JP17H06361 and JP17H06364, JSPS Core-to-Core Program A. Advanced Research Networks, JSPS Grantin-Aid for Scientific Research (S) 17H06133 and 20H05639 , JSPS Grant-in-Aid for Transformative Research Areas (A) 20A203: JP20H05854, the joint research program of the Institute for Cosmic Ray Research, University of Tokyo, National Research Foundation (NRF), Computing Infrastructure Project of Global Science experimental Data hub Center (GSDC) at KISTI, Korea Astronomy and Space Science Institute (KASI), and Ministry of Science and ICT (MSIT) in Korea, Academia Sinica (AS), AS Grid Center (ASGC) and the National Science and Technology Council (NSTC) in Taiwan under grants including the Rising Star Program and Science Vanguard Research Program, Advanced Technology Center (ATC) of NAOJ, and Mechanical Engineering Center of KEK.

REFERENCES

Aasi, J., et al. 2014, Class. Quantum Grav., 31, 165014, doi: 10.1088/0264-9381/31/16/165014

—. 2015, Class. Quantum Grav., 32, 074001, doi: 10.1088/0264-9381/32/7/074001

Abadie, J., et al. 2011, Nature Phys., 7, 962, doi: 10.1038/nphys2083

Abbott, B. P., et al. 2009, Rep. Prog. Phys., 72, 076901, doi: 10.1088/0034-4885/72/7/076901

—. 2016, Phys. Rev. Lett., 116, 061102

—. 2020a, Living Rev. Rel., 23, doi: 10.1007/s41114-020-00026-9

—. 2020b, ApJ Lett., 892, L3, doi: 10.3847/2041-8213/ab75f5

—. 2020c, Class. Quantum Grav., 37, 055002, doi: 10.1088/1361-6382/ab685e

—. 2021a, Phys. Rev. X, 11, 021053, doi: 10.1103/PhysRevX.11.021053

—. 2021b. https://arxiv.org/abs/2108.01045

—. 2021c, GWTC-3: Compact Binary Coalescences Observed by LIGO and Virgo During the Second Part of the Third Observing Run. https://arxiv.org/abs/2111.03606

—. 2021d, SoftwareX, 13, 100658, doi: https://doi.org/10.1016/j.softx.2021.100658

—. 2022, Progress of Theoretical and Experimental Physics, 2022, 063F01, doi: 10.1093/ptep/ptac073

Abbott, R., et al. 2020d, Phys. Rev. D, 102, 043015, doi: 10.1103/PhysRevD.102.043015

—. 2020e, Phys. Rev. Lett., 125, 101102, doi: 10.1103/PhysRevLett.125.101102

—. 2020f, ApJ Lett., 896, L44, doi: 10.3847/2041-8213/ab960f

—. 2021e, Phys. Rev. D, 104, 022004, doi: 10.1103/PhysRevD.104.022004

—. 2021f, Phys. Rev. D, 104, 022005, doi: 10.1103/PhysRevD.104.022005

—. 2021g, ApJ Lett., 915, L5, doi: 10.3847/2041-8213/ac082e

Abe, H., et al. 2022, Progress of Theoretical and Experimental Physics, ptac093, doi: 10.1093/ptep/ptac093

Acernese, F., et al. 2005, Class. Quantum Grav., 22, doi: 10.1088/0264-9381/22/18/S18

—. 2015, Class. Quantum Grav., 32, 024001, doi: 10.1088/0264-9381/32/2/024001

—. 2019, Phys. Rev. Lett., 123, 231108, doi: 10.1103/PhysRevLett.123.231108

—. 2022a. https://arxiv.org/abs/2205.01555

—. 2022b, Class. Quantum Grav., 39, 045006, doi: 10.1088/1361-6382/ac3c8e

—. 2022c. https://arxiv.org/abs/2210.15633

Akutsu, T., et al. 2016, Opt. Mater. Express, 6, 1613, doi: 10.1364/OME.6.001613

—. 2018, Progress of Theoretical and Experimental Physics, 2018, 013F01, doi: 10.1093/ptep/ptx180

—. 2021, Progress of Theoretical and Experimental Physics, 2021, 05A101, doi: 10.1093/ptep/ptaa125

Allen, B., & Romano, J. D. 1999, Phys. Rev. D, 59, 102001, doi: 10.1103/PhysRevD.59.102001

Ashton, G., et al. 2019, ApJS, 241, 27, doi: 10.3847/1538-4365/ab06fc

Astone, P., Colla, A., D'Antonio, S., Frasca, S., & Palomba, C. 2014, Phys. Rev. D, 90, 042002, doi: 10.1103/PhysRevD.90.042002

Aubin, F., et al. 2021, Class. Quantum Grav., 38, 095004, doi: 10.1088/1361-6382/abe913

Barsotti, L., Harms, J., & Schnabel, R. 2019, Rep. Prog. Phys., 82, 016905, doi: 10.1088/1361-6633/aab906

Biwer, C., et al. 2017, Phys. Rev. D, 95, 062002, doi: 10.1103/PhysRevD.95.062002

Buikema, A., et al. 2020, Phys. Rev. D, 102, 062003, doi: 10.1103/PhysRevD.102.062003

Callister, T. A., & Farr, W. M. 2023. https://arxiv.org/abs/2302.07289

Capano, C. D., Cabero, M., Westerweck, J., et al. 2021. https://arxiv.org/abs/2105.05238

Capano, C. D., Abedi, J., Kastha, S., et al. 2022. https://arxiv.org/abs/2209.00640

Chen, D., Naticchioni, L., Khalaidovski, A., et al. 2014, Class. Quantum Grav., 31, 224001, doi: 10.1088/0264-9381/31/22/224001

Chen, H.-Y., et al. 2021, Class. Quantum Grav., 38, 055010, doi: 10.1088/1361-6382/abd594

Cornish, N. J., Littenberg, T. B., Bécsy, B., et al. 2021, Phys. Rev. D, 103, 044006, doi: 10.1103/PhysRevD.103.044006

Davies, G. S., Dent, T., Tápai, M., et al. 2020, Phys. Rev. D, 102, 022004, doi: 10.1103/PhysRevD.102.022004

Davis, D., Littenberg, T. B., Romero-Shaw, I. M., et al. 2022, Class. Quantum Grav., 39, 245013, doi: 10.1088/1361-6382/aca238

Davis, D., et al. 2019, Class. Quantum Grav., 36, 055011, doi: 10.1088/1361-6382/ab01c5

—. 2021a, Class. Quantum Grav., 38, 135014, doi: 10.1088/1361-6382/abfd85

—. 2021b, Class. Quantum Grav., 38, 135014, doi: 10.1088/1361-6382/abfd85
Dooley, K. L., et al. 2016, Class. Quantum Grav., 33, 075009, doi: 10.1088/0264-9381/33/7/075009
Ellis, G. 2012, Control System Design Guide (Fourth Edition) (Butterworth-Heinemann), doi: 10.1016/C2010-0-65994-3
Essick, R., Godwin, P., Hanna, C., Blackburn, L., & Katsavounidis, E. 2020, Mach. Learn.: Sci. Technol., 2, 015004, doi: 10.1088/2632-2153/abab5f
Estellés, H., et al. 2022, ApJ, 924, 79, doi: 10.3847/1538-4357/ac33a0
Estevez, D., Mours, B., Rolland, L., & Verkindt, D. 2019. https://tds.virgo-gw.eu/ql/?c=14486
Finn, L. S., & Chernoff, D. F. 1993, Phys. Rev. D, 47, 2198, doi: 10.1103/PhysRevD.47.2198
Fisher, R. P., Hemming, G., Bizouard, M.-A., et al. 2021, SoftwareX, 14, 100677, doi: 10.1016/j.softx.2021.100677
Glanzer, J., et al. 2023, Class. Quantum Grav., 40, 065004, doi: 10.1088/1361-6382/acb633
Harris, C. R., et al. 2020, Nature, 585, 357, doi: 10.1038/s41586-020-2649-2
Hoy, C., & Raymond, V. 2021, SoftwareX, 15, 100765, doi: 10.1016/j.softx.2021.100765
Hunter, J. D. 2007, Comput. Sci. Eng., 9, 90, doi: 10.1109/MCSE.2007.55
John Zweizig. 2006, The Data Monitor Tool Project, labcit.ligo.caltech.edu/~jzweizig/DMT-Project.html
Klimenko, S., Vedovato, G., Drago, M., et al. 2016, Phys. Rev. D, 93, 042004, doi: 10.1103/PhysRevD.93.042004
Koziol, Q., & Robinson, D. 2018, HDF5. https://doi.org/10.11578/dc.20180330.1
Krishnan, B., Sintes, A. M., Papa, M. A., et al. 2004, Phys. Rev. D, 70, 082001, doi: 10.1103/PhysRevD.70.082001
LIGO Laboratory. 2022a. https://dcc.ligo.org/LIGO-M1000066/public
—. 2022b, doi: 10.7935/38s2-7g84
LIGO Scientific Collaboration. 2018, LIGO Algorithm Library, doi: 10.7935/GT1W-FZ16
LIGO Scientific Collaboration, & Virgo Collaboration. 2021, LIGO and Virgo Calibration Uncertainty (O1, O2 and O3), v3. https://dcc.ligo.org/T2100313/public
LIGO Scientific Collaboration and Virgo Collaboration. 2009, Specification of a Common Data Frame Format for Interferometric Gravitational Wave Detectors, Tech. Rep. VIR-067A-08. https://dcc.ligo.org/LIGO-T970130/public
—. 2016, Data quality vetoes applied to the analysis of GW150914. https://dcc.ligo.org/LIGO-T1600011/public
—. 2018, Data quality report user documentation, docs.ligo.org/detchar/data-quality-report/
—. 2019. https://dcc.ligo.org/LIGO-M060038/public
—. 2021a, doi: 10.7935/nfnt-hm34
—. 2021b, doi: 10.7935/pr1e-j706
—. 2021c, GWTC-2.1: Deep Extended Catalog of Compact Binary Coalescences Observed by LIGO and Virgo During the First Half of the Third Observing Run - Candidate Data Release, v3, Zenodo, doi: 10.5281/zenodo.5759108
—. 2021d, GWTC-2.1: Deep extended-catalog of Compact Binary Coalescences Observed by LIGO and Virgo During the First Half of the Third Observing Run - Sensitivity of search pipelines to simulated signals, Zenodo, doi: 10.5281/zenodo.5117799
—. 2022a, GWTC-2.1: Deep Extended Catalog of Compact Binary Coalescences Observed by LIGO and Virgo During the First Half of the Third Observing Run - Data Quality Products for GW Searches, Zenodo, doi: 10.5281/zenodo.6477646
—. 2022b, GWTC-2.1: Deep Extended Catalog of Compact Binary Coalescences Observed by LIGO and Virgo During the First Half of the Third Observing Run - Parameter Estimation Data Release, Zenodo, doi: 10.5281/zenodo.6513631
—. 2022c, GWTC-2.1: Deep Extended Catalog of Compact Binary Coalescences Observed by LIGO and Virgo During the First Half of the Third Observing Run - Glitch modelling for events, Zenodo, doi: 10.5281/zenodo.6477076
LIGO Scientific Collaboration, Virgo Collaboration and KAGRA Collaboration. 2021a, GWTC-3: Compact Binary Coalescences Observed by LIGO and Virgo During the Second Part of the Third Observing Run — Candidate data release, Zenodo, doi: 10.5281/zenodo.5546665
—. 2021b, GWTC-3: Compact Binary Coalescences Observed by LIGO and Virgo During the Second Part of the Third Observing Run — O3 search sensitivity estimates, Zenodo, doi: 10.5281/zenodo.7890437
—. 2021c, GWTC-3: Compact Binary Coalescences Observed by LIGO and Virgo During the Second Part of the Third Observing Run — Data Quality Products for GW Searches, Zenodo, doi: 10.5281/zenodo.5636796
—. 2021d, GWTC-3: Compact Binary Coalescences Observed by LIGO and Virgo During the Second Part of the Third Observing Run — Parameter estimation data release, Zenodo, doi: 10.5281/zenodo.5546663

—. 2021e, GWTC-3: Compact Binary Coalescences Observed by LIGO and Virgo During the Second Part of the Third Observing Run — Glitch modelling for events, Zenodo, doi: 10.5281/zenodo.5546680

—. 2021f, Data distribution of Constraints on the cosmic expansion history from the GWTC-3, Zenodo, doi: 10.5281/zenodo.5645777

—. 2022a, doi: 10.7935/38s2-7g84

—. 2022b. https://observing.docs.ligo.org/plan

—. 2023a, GWTC-3: Compact Binary Coalescences Observed by LIGO and Virgo During the Second Part of the Third Observing Run — O1+O2+O3 Search Sensitivity Estimates, Zenodo, doi: 10.5281/zenodo.7890398

—. 2023b, The population of merging compact binaries inferred using gravitational waves through GWTC-3 - Data release, Zenodo, doi: 10.5281/zenodo.7843926

Lough, J., et al. 2021, Phys. Rev. Lett., 126, 041102, doi: 10.1103/PhysRevLett.126.041102

Lyu, Z., Jiang, N., & Yagi, K. 2022, Phys. Rev. D, 105, 064001, doi: 10.1103/PhysRevD.105.064001

Macleod, D., et al. 2021a, gwpy/gwsumm, Zenodo, doi: 10.5281/zenodo.4975045

—. 2021b, gwpy/gwpy, Zenodo, doi: 10.5281/zenodo.597016

Macleod, D. M., Areeda, J. S., Coughlin, S. B., Massinger, T. J., & Urban, A. L. 2021c, SoftwareX, 13, 100657, doi: https://doi.org/10.1016/j.softx.2021.100657

Mukund, N., Lough, J., Affeldt, C., et al. 2020, Phys. Rev. D, 101, 102006, doi: 10.1103/PhysRevD.101.102006

Nitz, A. H., Kumar, S., Wang, Y.-F., et al. 2023, ApJ, 946, 59, doi: 10.3847/1538-4357/aca591

Nitz, A. H., & Wang, Y.-F. 2022, Phys. Rev. D, 106, 023024, doi: 10.1103/PhysRevD.106.023024

Nyquist, H. 1924, Bell System Technical Journal, 3, 324, doi: 10.1002/j.1538-7305.1924.tb01361.x

Olsen, S., Venumadhav, T., Mushkin, J., et al. 2022, Phys. Rev. D, 106, 043009, doi: 10.1103/PhysRevD.106.043009

Périgois, C., Mapelli, M., Santoliquido, F., Bouffanais, Y., & Rufolo, R. 2023. https://arxiv.org/abs/2301.01312

Robinet, F., Arnaud, N., Leroy, N., et al. 2020, SoftwareX, 12, 100620, doi: 10.1016/j.softx.2020.100620

Rolland, L., Seglar-Arroyo, M., & Verkindt, D. 2019. https://tds.virgo-gw.eu/ql/?c=15041

Roulet, J., Chia, H. S., Olsen, S., et al. 2021, Phys. Rev. D, 104, 083010, doi: 10.1103/PhysRevD.104.083010

Sachdev, S., et al. 2019. https://arxiv.org/abs/1901.08580

Sathyaprakash, B. S., & Schutz, B. F. 2009, Living Rev. Rel., 12, 2, doi: 10.12942/lrr-2009-2

Schnabel, R., Mavalvala, N., Mc Clelland, D. E., & Lam, P. K. 2010, Nat. Commun., 1, 121, doi: 10.1038/ncomms1122

Smith, J. R., Abbott, T., Hirose, E., et al. 2011, Class. Quantum Grav., 28, 235005, doi: 10.1088/0264-9381/28/23/235005

Steltner, B., Papa, M. A., Eggenstein, H. B., et al. 2023. https://arxiv.org/abs/2303.04109

Sun, L., et al. 2020, Class. Quantum Grav., 37, 225008, doi: 10.1088/1361-6382/abb14e

—. 2021. https://arxiv.org/abs/2107.00129

Tse, M., et al. 2019, Phys. Rev. Lett., 123, 231107, doi: 10.1103/PhysRevLett.123.231107

Urban, A., et al. 2021, gwdetchar/gwdetchar, Zenodo, doi: 10.5281/zenodo.597016

Vajente, G., et al. 2020a, Phys. Rev. D, 101, 042003, doi: 10.1103/PhysRevD.101.042003

—. 2020b, Phys. Rev. D, 101, 042003, doi: 10.1103/PhysRevD.101.042003

Viets, A., et al. 2018, Class. Quantum Grav., 35, 095015, doi: 10.1088/1361-6382/aab658

Virtanen, P., et al. 2020, Nature Meth., 17, 261, doi: 10.1038/s41592-019-0686-2

Wang, Y.-F., Brown, S. M., Shao, L., & Zhao, W. 2022, Phys. Rev. D, 106, 084005, doi: 10.1103/PhysRevD.106.084005

Waskom, M. 2021, J. Open Source Softw., 6, doi: 10.21105/joss.03021

Weisberg, J. M., & Huang, Y. 2016, ApJ, 829, 55, doi: 10.3847/0004-637X/829/1/55

Weitzel, D., Bockelman, B., Brown, D. A., et al. 2017, in Proceedings of the Practice and Experience in Advanced Research Computing 2017 on Sustainability, Success and Impact No. 24, doi: 10.48550/arXiv.1705.06202

Whelan, J. T., et al. 2023. https://arxiv.org/abs/2302.10338

Zweizig, Z., Maros, E., Hanks, J., & Areeda, J. 2021. https://wiki.ligo.org/Computing/NDSClient/